Advances in Quantifying Air-Sea Gas Exchange and Environmental Forcing*

Rik Wanninkhof,[1] William E. Asher,[2] David T. Ho,[3] Colm Sweeney,[4] and Wade R. McGillis[5]

[1]National Oceanographic and Atmospheric Administration/Atlantic Oceanographic and Meteorological Laboratory, Miami, Florida 33149; email: Rik.Wanninkhof@noaa.gov

[2]Applied Physics Laboratory, University of Washington, Seattle, Washington 98105; email: asher@apl.washington.edu

[3]Department of Oceanography, University of Hawaii, Honolulu, Hawaii 96822; email: david.ho@hawaii.edu

[4]Global Monitoring Division, National Oceanographic and Atmospheric Administration/Earth Systems Research Laboratory, Boulder, Colorado 80305; email: Colm.Sweeney@noaa.gov

[5]Lamont-Doherty Earth Observatory of Columbia University, Palisades, New York 10964; email: wrm2102@columbia.edu

Annu. Rev. Mar. Sci. 2009. 1:213–44

First published online as a Review in Advance on September 19, 2008

The *Annual Review of Marine Science* is online at marine.annualreviews.org

This article's doi:
10.1146/annurev.marine.010908.163742

1941-1405/09/0115-0213$20.00

Key Words

gas fluxes, gas transfer velocity, carbon cycle, air-sea interaction

Abstract

The past decade has seen a substantial amount of research on air-sea gas exchange and its environmental controls. These studies have significantly advanced the understanding of processes that control gas transfer, led to higher quality field measurements, and improved estimates of the flux of climate-relevant gases between the ocean and atmosphere. This review discusses the fundamental principles of air-sea gas transfer and recent developments in gas transfer theory, parameterizations, and measurement techniques in the context of the exchange of carbon dioxide. However, much of this discussion is applicable to any sparingly soluble, non-reactive gas. We show how the use of global variables of environmental forcing that have recently become available and gas exchange relationships that incorporate the main forcing factors will lead to improved estimates of global and regional air-sea gas fluxes based on better fundamental physical, chemical, and biological foundations.

INTRODUCTION

Air-sea gas exchange has been of intensive scientific interest for more than half a century because of its importance in biogeochemical cycling of climate, weather, and health-related gaseous compounds. In particular, gas exchange contributes to the mitigation of the anthropogenic greenhouse effect through absorption of excess atmospheric CO_2 by the oceans. Gas exchange is also important to climate and atmospheric radiative transfer because of the sea-to-air flux of dimethylsulfide (DMS), which serves as a precursor to cloud condensation nuclei (CCN). CCN, in turn, are involved in radiative forcing through direct and indirect aerosol effects (Forster et al. 2007). In addition, oxygen levels in ocean surface waters are critically dependent on air-sea gas exchange, and the invasion of O_2 can alleviate hypoxia in coastal oceans and estuaries. On local and regional scales, the fate of volatile pollutants also depends on air-water gas exchange.

The study of air-sea gas exchange is multifaceted. Understanding exchange processes at the molecular level has improved our understanding of how environmental factors control the rate of exchange at the air-water interface. Some of the first studies on transfer across liquid-gas surfaces were focused on industrial applications (see, for instance, Danckwerts 1970). For environmental applications, a significant effort has been devoted to techniques for determining gas transfer rates, processes that control them, and theories and techniques to quantify gas fluxes. For determination of gas exchange over the ocean, many efforts have been of an opportunistic nature and take advantage of O_2 disequilibria that arise from biological productivity (Redfield 1948) or utilize ^{14}C excesses in the atmosphere from nuclear bomb tests, called bomb ^{14}C, that invaded the ocean (Broecker et al. 1985, 1995; Sweeney et al. 2007). Of particular note are the improvements in meteorological flux techniques that measure air-sea gas fluxes in the atmsopheric boundary layer on minute timescales (McGillis et al. 2001) and waterside, deliberate tracer techniques that can provide gas exchange estimates in the field with timescales on the order of 24 h (Ho et al. 2006). However, much of the interest in gas fluxes over the ocean relates to regional or global phenomena that occur over seasonal to decadal timescales such that upscaling of field studies is a major consideration. Upscaling involves relating gas transfer to the environmental factors that influence the exchange (**Figure 1**). Most commonly, upscaling is accomplished by relating gas transfer to wind speed (Wanninkhof 1992). The upscaling is challenging because of uncertainties in the relationship between gas exchange and wind speed, biases in different wind speed products, and issues with ignoring the cross correlations between gas transfer and wind. There is also increasing evidence that gas transfer cannot be adequately quantified with wind speed alone. Several studies have shown that other effects such as surface films (Broecker et al. 1978; Asher & Pankow 1986; Frew et al. 1990, 2004; Frew 1997; Asher 1997; Bock et al. 1999; Saylor & Handler 1999; Zappa et al. 2001, 2004; Tsai & Liu 2003), bubble entrainment (Monahan & Spillane 1984, Wallace & Wirick 1992, Farmer et al. 1993, Asher et al. 1996, Zhang et al. 2006, McNeil & d'Asaro 2007), rain (Ho et al. 1997, 2004; Takagaki & Komori 2007), and boundary layer stability (Erickson 1993) can affect the gas transfer process.

We report on recent findings to update several excellent reviews of air-sea gas transfer (Liss 1983, Liss & Merlivat 1986, Liss et al. 1988, Jähne & Haußecker 1998) and books and special journal volumes on gas exchange (Brutsaert & Jirka 1984, Wilhelms & Gulliver 1991, Jähne & Monahan 1995, Liss & Duce 1997, Donelan et al. 2002, McGillis et al. 2004a, Borges & Wanninkhof 2007, Garbe et al. 2007). We start with a brief description of basic principles, followed by an overview of measurement techniques. Several different approaches are available to quantify gas transfer, ranging from laboratory studies to global perturbations. We discuss gas exchange models based on physical forcing, both with respect to their applications and to the issues and veracity in developing such models. The last sections focus on developing hybrid gas transfer models and their application to global air-sea CO_2 fluxes.

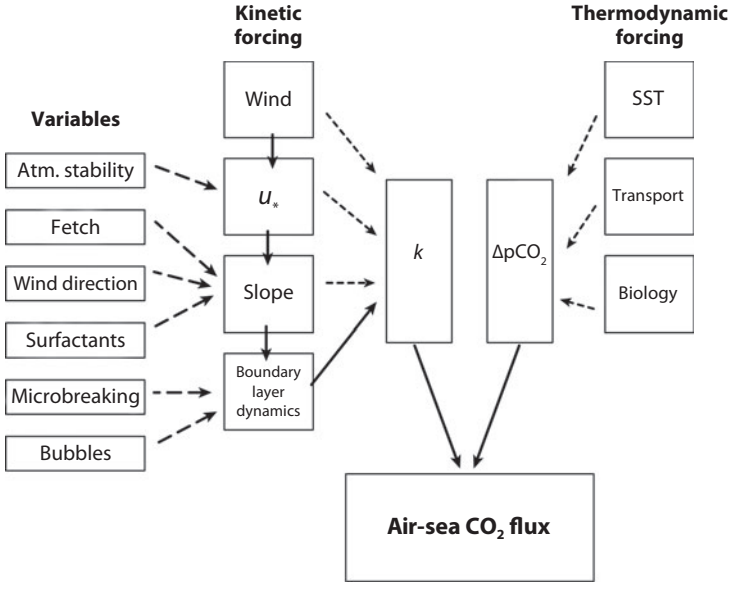

Figure 1

Simplified schematic of factors that affect air-sea CO_2 fluxes. On the left are environmental forcing factors (kinetic forcing) that control the gas transfer velocity, k, and the variables that influence the forcing. On the right are the factors that affect the air-sea pCO_2 difference (thermodynamic forcing, see Equation 3), also called thermodynamic driving potential.

BASIC PRINCIPLES

The flux of slightly soluble nonreactive gases across the air-sea interface, F[1] (mol $m^{-2}s^{-1}$), can be defined as the product of a quantity called the gas transfer velocity, k (m s^{-1}), and the concentration difference between the top and bottom of the liquid boundary layer,

$$F = k(C_w - C_o), \tag{1}$$

where C_o is the gas concentration at the water surface (mol m^{-3}) and C_w is the gas concentration in the well-mixed bulk fluid below (mol m^{-3}). The gas transfer velocity is referred to as the kinetic forcing function, and the concentration difference is the thermodynamic driving potential (**Figure 1**). Assuming equivalence of chemical potential across the air-water phase boundary, C_o is expressed in terms of the concentration of the gas in the air, C_a (mol m^{-3}), and the dimensionless Ostwald solubility coefficient α. Under this assumption, Equation 1 becomes

$$F = k(C_w - \alpha C_a), \tag{2}$$

where by convention F is negative for a flux of gas from the atmosphere to the ocean. Often, Equation 2 is written such that the thermodynamic driving force is expressed in terms of the partial pressure of the gas in air and water. In the case of CO_2, exchange across the air-water interface (Equation 2) is

$$F = k K_o(pCO_{2w} - pCO_{2a}), \tag{3}$$

[1]For a complete list of symbols used in this article, please see Appendix A.

where K_o (mol m^{-3} Pa^{-1}) is the aqueous-phase solubility of CO_2, pCO_{2a} (Pa) is the partial pressure of CO_2 in air, and pCO_{2w} (Pa) is the partial pressure of CO_2 in water. Assuming CO_2 behaves as an ideal gas, K_o is related to α by $K_o = \alpha\ (R\ T_W)^{-1}$, where R (m^3 Pa K^{-1} mol^{-1}) is the ideal gas constant and T_W (K) is the water temperature. For sparingly soluble gases that are subject to rapid chemical reaction in the aqueous phase (for instance, the air-water exchange of CO_2 for pH > 10), Equation 2 must be modified as

$$F = k\varepsilon\,(C_w - \alpha\ C_a), \tag{4}$$

where ε is the chemical enhancement factor.

Although the parameterizations for k discussed below are largely empirical in nature, providing a conceptual model for air-sea gas transfer aids in both understanding which environmental forcings are most important and in relating gas transfer measurements made using one gas (for instance, ^{222}Rn) to a different gas (for instance, CO_2) on the basis of the physicochemical properties of the gases. Nearly all conceptual models for air-water transfer of slightly soluble (that is, $\alpha <\approx 5$), nonreactive gases show that k is controlled by the aqueous-phase hydrodynamics very near the air-water interface. The simplest of these is the stagnant-film model (Liss & Slater 1974), which proposes that the transfer process is rate limited by molecular diffusion through a thin layer of water with constant thickness at the air-water interface. From Fick's first law of diffusion, k is then equal to molecular diffusivity, D (m^2 s^{-1}), divided by the thickness of the stagnant film, δ (m). Therefore, processes that decrease δ will increase k.

Although appealing in its simplicity, stagnant-film theory is lacking because it does not provide a complete physical picture of the transfer process. For example, laboratory and field studies have shown that k is better modeled as being proportional to D to a fractional power between one-half and two-thirds (Ledwell 1984, Jähne et al. 1984, Upstill-Goddard et al. 1990, Nightingale et al. 2000b). Although this discrepancy can be resolved through scaling arguments that suggest that δ is proportional to $D^{1/2}$ or $D^{1/3}$ (Davies 1972) so that the ratio of D/δ has the observed functionality with respect to k, direct and indirect measurements of the gas concentrations very near the water surface have shown that the near surface is poorly modeled as a stagnant layer with constant thickness (Lee & Luk 1982, Luk & Lee 1986, Asher & Pankow 1989, Wolff & Hanratty 1994, Münsterer & Jähne 1998, Woodrow & Duke 2001, Takehara & Etoh 2002). A more accurate conceptual model envisions the near-surface layer as dynamic, either with a variable thickness controlled by impinging eddies (Harriott 1962), flow divergences (Brumley & Jirka 1988), or mixing with the bulk at frequent intervals through surface renewal events (Danckwerts 1951). These more complex models predict that k will be proportional to D to a fractional power between one-half and two-thirds, in agreement with the experimental results (for instance, Davies et al. 1964). Understanding the dependence of k on D is critical because there is a very limited number of gases suitable for use as tracers of the air-sea gas flux and, in many cases, the gas for which F must be known cannot be measured directly. Thus, measurements of F made for one gas must be converted into the F for the gas of interest. Typically, this is done by using a predicted functional relationship between D and k to convert between k for two different gases. Development of accurate parameterizations of air-sea exchange that are applicable for a range of gases must include the dependence of k on D.

A complete exposition of the range of conceptual models available for air-sea gas exchange is beyond the scope of this review. However, one similar feature of these models is they predict that k will be proportional to D^n where $1/2 < n < 2/3$, depending on the assumptions made about the details of the hydrodynamics in the near-surface aqueous layer and whether an eddy diffusion/boundary layer framework is adopted (for instance, Deacon 1977; Ledwell 1984; McCready & Hanratty 1984, 1985; Jähne et al. 1987; Brumley & Jirka 1988; Fairall et al. 2000; Banerjee et al.

2004; Hara et al. 2007) or an eddy structure approach such as surface renewal or surface penetration is used (Danckwerts 1951, Harriott 1962, Fortescue & Pearson 1967, Lamont & Scott 1970, Soloviev & Schlussel 1994, Zhao et al. 2003). These approaches all share a common detail that k is expressed in terms of the molecular diffusivity and some function based on the aqueous-phase hydrodynamics or characteristics of the aqueous boundary layer. This can be written as

$$k = a\,D^n g(Q, L, \nu), \tag{5}$$

where a is a constant that is model dependent and $g(Q, L, \nu)$ represents a model-dependent function based on a velocity scale, Q (for instance, the turbulence intensity, water-side friction velocity u_*), a length scale, L (for instance, turbulence integral length scale, boundary layer depth), and the kinematic viscosity of water, ν. Typically, Equation 5 is modified in terms of the nondimensional Schmidt number (Sc) (defined as $\mathrm{Sc} = \nu/D$) so that k becomes

$$k = a\mathrm{Sc}^{-n} f(Q, L, \nu). \tag{6}$$

The parameterizations of k presented below are all derived empirically from this functional form based on the assumption that the kinetic energy input to the water from the wind stress is fundamental in driving air-water exchange. Because the energy input from the wind is known to increase nonlinearly with wind speed owing to wave generation and wave breaking (for instance, Craig & Banner 1994, Terray et al. 1996), parameterizations of k in terms of wind speed, U, propose that k will increase in proportion to U^m where $\mathrm{m} > 1$, a conclusion that has been supported by laboratory and field results.

It should be noted that Equation 6 is not appropriate for expressing the transfer rate for soluble or reactive gases. The rate of transfer of gases with $\alpha > 100$, or gases that rapidly react in water, is not controlled by hydrodynamic processes in the water side of the air-water interface (Liss & Slater 1974). Instead, k for these gases is controlled by air-side processes (**Figure 2**). Gases of environmental interest that fall in this category include water vapor, ozone, ammonia, and sulfur dioxide. Limited studies performed with soluble gases show transfer velocities that are two to three orders of magnitude higher than nonsoluble gases at a given U, and the functionality with respect to U is nearly linear (Liss 1983, Gallagher et al. 2001, Chang et al. 2004, McGillis et al. 2007). Gases with intermediate solubility exhibit both air-side and water-side resistance. For instance, DMS with $\alpha \approx 10$ is approximately 10% air-phase and 90% water-phase controlled (McGillis et al. 2000). A summary of D, Sc, and α values for select gases of environmental interest at 20°C in seawater is given in **Table 1**.

Whether a gas will be rate controlled in the air or water is most easily described in terms of the two-film model by Liss & Slater (1974). The total resistance to transfer is then the sum of the air and water resistances, and k is inversely proportional to the total resistance,

$$k^{-1} = (k_a/\alpha)^{-1} + (\varepsilon k_w)^{-1}, \tag{7}$$

where k_a/α ($= 1/R_{air}$ with R_{air} as the air-side resistance) and εk_w ($= 1/R_{water}$ with R_{water} as the water-side resistance) are the gas transfer velocities of the gas through the diffusive sublayer layers in the air-side and water-side of the interface, respectively. On the basis of the two-film model, k_a and k_w are roughly proportional to the ratio of D for the gas in air and water so that $k_a \approx 100\,k_w$. Therefore, the water phase and air phase resistance will be roughly equal if $\varepsilon\alpha \approx 100$.

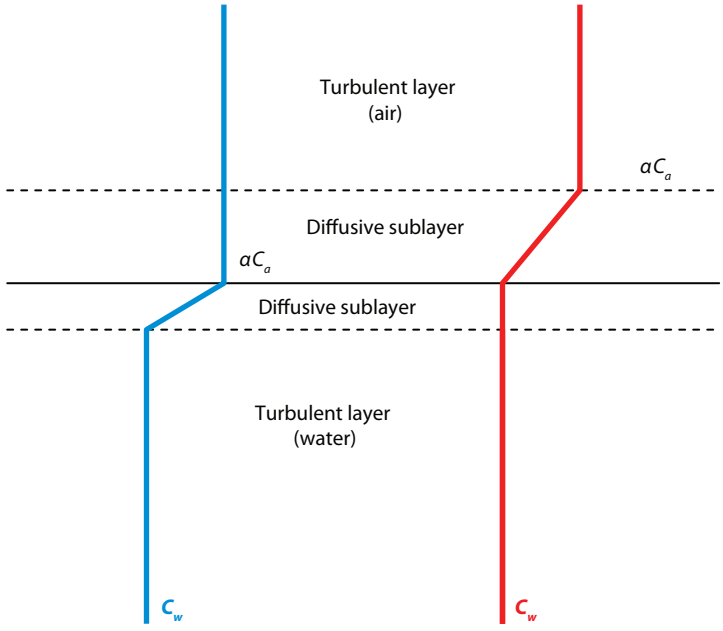

Figure 2

Conceptual view of boundary layer concentration profiles where the resistance to gas transfer is concentrated in the diffusive sublayers. On the left (*blue line*) is the concentration profile for an insoluble gas with the resistance in the aqueous-side diffusive sublayer. On the right (*red line*) is the profile for a soluble gas with resistance in the air-side diffusive sublayer. Soluble gases have an Ostwald solubility $\approx > 100$.

MEASUREMENT TECHNIQUES

As described above, the k for CO_2, k_{CO_2}, can be determined from other gases through their Sc number dependence. The measurement of gas transfer velocities and fluxes can be separated into to three broad categories:

1. Measurement of F in the air above the sea surface and ΔC in the water to determine k using Equation 1. These methods are referred to as direct flux measurements or micrometeorological approaches and include covariance (or eddy correlation), eddy accumulation, atmospheric concentration profile, and inertial dissipation techniques.
2. Measurement of C_a (in air) and the change in C_w (in water) as a function of time. Assuming the water volume and surface area are known, F is then equal to the change in C_w multiplied by the ratio of the volume to the surface area. Then, k can be calculated with C_a and C_w using Equation 1. These bulk concentration techniques include mass-balance and perturbation studies where the concentration of gases in air and water are out of equilibrium through biological consumption/production, water heating/cooling (N_2, O_2, CO_2, noble gases), radioactive decay (^{222}Rn), or by purposeful addition (^3He, SF_6).
3. Proxy techniques where a nongaseous tracer whose air-sea flux is more easily measured is used as a surrogate for a gas using the principle that all air-water transfer is controlled by the near-surface hydrodynamics. In field applications, proxy methods are limited to thermographic methods that use heat.

The mathematical formalism, application, merits, and drawbacks of each method are outlined below. The assessment focuses on the challenges, but progress has been significant over

Table 1 Diffusion coefficients, Schmidt numbers (Sc), and solubilities for select gases at 20°C for salt water (S = 35‰)[1]

Gas	Mol. weight (g mol^{-1})	D (10^{-5} cm^2 s^{-1})	Sc	α	Comment
^{3}He	3	7.29	144	0.008	≈1% less soluble than He
He	4	6.36	165	0.008	
CH_4	16	1.55	677	0.028	
Ne	20	3.33	315	0.009	
N_2	28	1.57	670	0.012	
O_2	32	1.78	589	0.025	
Ar	40	1.82	576	0.028	
CO_2	44	1.59	660	0.727	
N_2O	44	1.5	698	0.524	
$(CH_3)_2S$	62	1.14	918	12.73	DMS
Kr	84	1.51	694	0.050	
CCl_2F_2	121	0.86	1219	0.09	CFC-12
Xe	131	1.19	880	0.1	
CCl_3F	137	0.94	1120	0.31	CFC-11
SF_6	146	1.05	992	0.004	
CCl_4	154	0.82	1286	0.68	
CCl_2FCClF_2	187	0.68	1544	0.1	CFC-113
Rn	222	1.07	980	0.317	
Heat	—	1.75	6	—	

[1]Values are from disparate sources and should be considered approximate (≈5%).

the past decade, and the new and improved techniques have improved our in situ capabilities to determine k .

Direct Flux Measurements

The first successful direct flux measurements for CO_2 from ships were performed in the late 1990s (McGillis et al. 2001). Detailed overviews of the direct flux techniques in air and applications can be found in McGillis et al. (2001) and Fairall et al. (2000). Brief synopses of these works are provided here.

Covariance technique. The covariance or eddy correlation technique is considered one of the purest ways to determine F, because it does not rely on assumptions about gas properties or approximations concerning the turbulent structure of the atmospheric boundary layer. However, it is one of the more challenging flux measurements to make in the field owing to small signal-to-noise ratios, which result from a very small signal and non-ideal measurement conditions found at sea (Fairall et al. 2000). In the covariance method, F can be directly measured from the gas concentration, c, and the vertical velocity, w, in the atmospheric boundary layer using the expression

$$F = \langle c'w' \rangle + c\,w, \tag{8}$$

where the primes indicate fluctuations about a mean value denoted by the "⟨ ⟩." The second term is mean velocity (of dry air) to maintain the density of dry air in the presence of latent and sensible heat fluxes. Covariance flux systems have been used extensively to measure momentum and heat

fluxes (for instance, Fairall et al. 1997). The greatest challenges to implementing the covariance method at sea for trace gases are as follows: rapid, high-precision measurement of atmospheric gas concentrations; correction of the measured fluxes for the covarying flux of water vapor and temperature [that is, the Webb effect (Webb et al. 1980, Liu 2005)]; and contamination of the turbulent velocity record by platform motion and flow distortion around the platform. Because the signal-to-noise ratio is small in covariance flux measurements, the presence of an air-sea gas concentration difference large enough that fluctuations in C_a are significantly larger than the precision of the measurement technique is critical for the covariance method.

Although the covariance technique has been used routinely on fixed platforms for many years (for instance, Katsaros et al. 1987), including CO_2 measurements (Jacobs et al. 2002), routine open-ocean applications of this technique for the measurement of turbulent fluxes from research vessels (Fairall et al. 1997, Edson et al. 1998) have been made only in the past two decades. In particular, the measurement of the velocity components necessary to compute covariances is more difficult because the motion of the platform impacts the actual velocity measurements of the air. This motion contamination must, therefore, be removed before the fluxes can be computed. The resulting corrected wind velocity can then be used to compute the covariance fluxes. However, even if the platform motion is completely removed from the measured velocity, the accuracy of velocity estimates is influenced by flow distortion around the vessel.

The challenge in applying this technique to trace gases is the high sampling rate and high precision required to constrain c', which typically requires sampling at 2 Hz or greater, and the relatively small signal (concentration variations with high background values) for many trace gases. Typically, the required precision of c' is at least two orders of magnitude greater than that of the air-sea gradient. With such stringent precision requirements, compounding factors such as platform motion and high sensible and latent heat fluxes can bias velocity/gas concentration covariance flux estimates. Covariance flux measurements have been successfully implemented on seagoing vessels for CO_2, DMS, and O_3. For CO_2, the uncertainty is 2 mol m^{-2} $year^{-1}$ (Fairall et al. 2000). By comparison, the average current oceanic CO_2 uptake due to the anthropogenic CO_2 pertubation is about 0.5 mol m^{-2} $year^{-1}$. This illustrates that the current CO_2 direct flux measurements are limited to large CO_2 source or sink regions. In contrast, DMS is highly supersaturated over most of the ocean, and atmospheric concentrations are low, so the c' will be correspondingly larger than for CO_2, which improves the signal-to-noise ratio (Huebert et al. 2004, Blomquist et al. 2006). Uncertainty in DMS fluxes is estimated to be 15–20% for a one-hour measurement (Huebert et al. 2004). Ozone fluxes (Lenchow et al. 1982) are large owing to the high solubility and reactivity of ozone in surface water, which again facilitates the measurements. However, the solubility of DMS and the reactivity of O_3 do not make either of them perfect proxies for air-water exchange of CO_2 or other sparingly soluble gases.

Recently, covariance techniques have been proposed for the water mixed layer in rough seas (d'Asaro & McNeil 2007). The longer time and length scales of turbulence alleviate the high sampling rate requirements. However, it is unclear if the criteria for the method, such as isotropic turbulence, are met in the water column, although the initial results look promising. Further research in performing covariance measurements in water is needed.

Relaxed eddy accumulation. The eddy accumulation (EA) method was developed for gases for which concentration measurements in air could not be performed at the required frequency needed for covariance measurements. The method relies on measuring the concentration of gas in the updraft and downdraft separately and is expressed mathematically as

$$F = b\,\chi\,\sigma_w(C_{up} - C_{down}), \tag{9}$$

where σ_w is the standard deviation of vertical velocity and the coefficient $b\chi$ depends on the threshold and characteristic length scales of turbulence (Businger & Delaney 1990; Nie et al. 1995; Zemmelink et al. 2002, 2004). The experimental setup is comprised of an anemometer that can accurately measure the vertical component of the wind, which is connected to a valve that can selectively sample the gas in the net upward component (updraft) and downward component (downdraft) of the wind. The major technical challenge in EA is to accurately sample gas concentrations specifically from updrafts and downdrafts. EA instruments generally utilize a threshold velocity range between the updraft and downdraft velocities, which is not sampled to avoid ambiguity and bias in sampling. These methods are appealing because high sampling rates for gas concentrations are not required as in the covariance method, and it is possible to dry the airstream before gas sampling to eliminate the need to correct for density variations caused by water vapor and temperature (Webb et al. 1980, Liu 2005).

Other Direct Flux Measurement Techniques

Other direct flux measurement techniques such as the profile method and the inertial dissipation approach rely heavily on similarity theory and scaling arguments that are commonly referred to as the Monin Obukov Similarity Theory (MOST). A comprehensive overview of how MOST is applied to the determination of gas fluxes can be found in Fairall et al. (2000). Here we provide a rudimentary conceptual explanation of the methods.

Profile Method. The profile method takes advantage of small concentration gradients in air that result from a net flux into or out of the water. The flux is the product of friction velocity in air, u_{a*}, and the concentration gradient between heights z_1 and z_2 in the atmsopheric boundary layer, divided by a transfer resistance, $R_{1,2}$, between the heights of measurement (Roether 1983):

$$F = u_{a*}(C_{z1} - C_{z2})(R_{1,2})^{-1}. \tag{10}$$

Under neutral boundary conditions,

$$R_{1,2} = \kappa^{-1} \ln(z_2/z_1), \tag{11}$$

where κ is the Von Karman constant ($\approx$0.4). A detailed description of the profile method with the theoretical foundation, including approximations for stable and unstable boundary conditions, can be found in McGillis et al. (2001) and Edson et al. (2004). The profile technique in the atmosphere requires the use of MOST for stable and unstable boundary layers. For this discussion, the simplified formulas listed in Equation 10 and Equation 11 suffice to show that measurement heights are a determining factor for the precision of the measurement. The transfer resistance scales with the natural log of the difference in measurement height in air such that it is advantageous to get the first measurement close to the surface.

Because the atmospheric profile method relies on mean gradients in the boundary layer, it offers several advantages over other direct flux measurement techniques. Many gases cannot be measured at rates that are high enough for eddy correlation because most gas measurement techniques rely on slow procedures that can also smear the high-frequency response (for instance, owing to water vapor removal and "dead volumes" en route to mass spectrometric and/or in gas chromatographic sample cells).

There are several requirements for the atmospheric profile technique to provide accurate fluxes. The surface momentum and buoyancy fluxes must be controlling the flow, and the parameterizations become invalid when, for instance, surface waves and larger-scale processes influence the near-surface properties. In addition, a number of fundamental assumptions such as surface

homogeneity, stationarity, and turbulent kinetic energy balance are required. The correction for atmospheric stability is very close to those used for profiles measured over land (Edson et al. 2004). Because of the relatively small vertical gradients of trace atmospheric gases, the signal levels can be close to or less than the gas detection noise level. In addition, displacements of the air intake and instruments due to the motion of the ship are problematic owing to the nonlinear nature of the vertical gas gradient. The flow distortion may significantly modify the profile of the gas concentration that is required for the flux computation. Finally, small-scale ($\approx$<100 m) variations in air-sea fluxes can cause variability in air concentrations in the footprint of measurement, which compromises the technique.

All the direct flux techniques measure surface fluxes rather than k. The k can be determined from knowledge of the air-water concentration difference (see Equation 2), which requires knowledge of the footprint of the flux measurement. The footprint is the region over which the flux emanates and depends on the height of measurement and boundary layer stability (Businger & Delaney 1990). For a measurement at 10-m height, the footprint ranges from 100 m to 20 km, with the larger footprint applicable to stable boundary layer conditions. Thus, comprehensive measurements of surface water gas concentrations in the footprint are essential for robust k estimates from direct flux techniques.

Mass Balance Techniques

These methods rely on measuring the rate of concentration change due to air-sea gas transfer to equilibrium conditions after a perturbation of the gases in water. The basic principle can be gleaned from Equation 2 and, recognizing that in the case where water volume exposed to the atmosphere is constant, F equals the change in mass of gas, M, divided by the surface area, A,

$$F = \partial M/\partial t \mathrm{A}^{-1}. \tag{12}$$

Thus, F can be determined and k can be estimated if the air-water concentration difference and mass decrease over time is known and well characterized. Several different methods of concentration perturbation can be utilized.

Natural perturbations (oxygen and radon). The first estimates of gas transfer in the ocean (embayments) were performed with O_2, taking advantage of disequilibria caused by temperature change or biological production and consumption (Redfield 1948). From changes in C_w for O_2 over time, the total change in mass of water volume exposed to the atmosphere is determined. The change in mass due to the air-sea flux (F_{O_2}) and with sources or sinks other than the air-sea flux (S) can be expressed as

$$F_{O_2} + S_{O_2} = \partial M/\partial t \mathrm{A}^{-1}. \tag{13}$$

The key is to adequately constrain S, which is often the largest source of uncertainty in such measurements. The flux estimate for O_2 based on changes in temperature of the water, in the absence of biological productivity, can often be determined more accurately because the temperature dependence of solubility of the gases is well known. The driving force for gas transfer in this case is the change in equilibrium due to changes in the αC_a term in Equation 2. Although C_a for oxygen is constant as far as gas transfer is concerned, changes in α with temperature will change C_o in Equation 1. Regional gas transfer velocities of O_2 have been estimated by this approach through the use of global numerical models (Najjar & Keeling 1997).

Radon has been used extensively for determination of gas exchange rates over the ocean because it has an accurately defined single loss (sink) term due to radioactive decay (Peng et al. 1979,

Smethie et al. 1985). In short, in the absence of gas transfer the ^{222}Rn gas will be in equilibrium with its parent, ^{226}Ra, in terms of activity, which is what is observed below the surface water mixed layer. Within the water mixed layer, some of the ^{222}Rn will escape owing to gas transfer such that the magnitude of disequilibrium of ^{222}Rn and ^{226}Ra in the mixed layer is directly proportional to the gas transfer rate. The pertinent equations to determine the gas transfer velocity are derived from Equation 2,

$$F_{^{222}\mathrm{Rn}} = k(^{222}\mathrm{Rn}_w - \alpha\,^{222}\mathrm{Rn}_a) \approx k(^{222}\mathrm{Rn}_w). \tag{14}$$

Here, the concentration of ^{222}Rn in the atmosphere is assumed to be zero. If the system is in steady state (stationary and homogeneous conditions in the water mixed layer), the loss due to radioactive decay must equal the flux

$$F_{^{222}\mathrm{Rn}} = \lambda I, \tag{15}$$

where λ is the decay constant (2.1 10^{-6} s^{-1} or 0.18 day^{-1}) and I is the deficit of ^{222}Rn relative to ^{226}Ra in the mixed layer (in terms of activity, A) such that $k = \lambda I / A_{^{222}\mathrm{Rnw}}$.

The response time of the method will be directly proportional to the half-life of ^{222}Rn of four days. Several large-scale ocean surveys and process studies have been performed to determine the gas transfer velocity with radon (Peng et al. 1979, Kromer & Roether 1983). Although basin-scale averages are in accord with other estimates, no clear relationship with wind was observed. Kromer & Roether (1983) provide a critical analysis of the uncertainties in the ^{222}Rn methods and guidelines for how an optimal ^{222}Rn gas exchange study in the ocean should be performed.

As with all mass balance techniques, gas exchange versus wind relationships with radon and oxygen are confounded by variability in two very important variables. The first is mixed layer depth, because changes in mixed layer depth will effectively change the mass, M, exposed to surface A (Equation 12). Regions with large gradients below the mixed layer will respond to changes in the mixed layer depth due to entrainment, with episodic shifts in surface concentration that may not be reflected in one-time concentration profiles in the water column. The second variable is shifts in wind speed over the course of the observation. Again, instantaneous observations of wind speed have often been used to calculate gas exchange using radon when it would be more appropraite to compare a weighted distribution of wind approximately two weeks prior to measuring the radon profile.

Deliberate tracers. Several of the shortcomings of the natural tracer methods, such as accounting for biological processes, can be alleviated by purposefully injecting a tracer gas into the water. Sulfur hexafluoride (SF_6) has been the tracer of choice because of its low level of detection and its relative ease of analysis (Upstill-Goddard et al. 1991, Wanninkhof et al. 1991). SF_6 is inert and present in water at very low concentrations, thus yielding an excellent signal-to-noise ratio. The SF_6 tracer method has been extensively used to estimate gas transfer in contained systems such as lakes and wind tunnels where the decrease of total mass of tracer can be accurately determined and used to estimate the gas transfer velocity. In a fixed water volume exposed to the atmosphere, where the air-phase concentration of SF_6 can be approximated as zero, use of Equation 1 shows the time rate of change in the aqueous-phase concentration of SF_6 can be written as

$$\frac{d\,[\mathrm{SF}_{6w}]}{dt} = \frac{AF_{\mathrm{SF6}}}{V} = -\frac{k\,(\mathrm{SF}_{6w})}{h}\,[\mathrm{SF}_{6w}]\,, \tag{16}$$

where A is the surface area, V is the water volume, h is the mixed layer depth defined as V/A, and $[SF_{6w}]$ is the concentration of SF_6 in water. Equation 16 can be integrated from time t_1 to time t_2

and rearranged to yield

$$k\,(\mathrm{SF}_6) = -\frac{h}{\Delta t}\ln\left(\frac{[\mathrm{SF}_{6w}]_{t2}}{[\mathrm{SF}_{6w}]_{t1}}\right), \tag{17}$$

where $\Delta t = t_2 - t_1$. Thus, k can be determined from the change in natural log of $[\mathrm{SF}_{6w}]$ over time, provided h is known.

For the open ocean, the decrease in (SF_{6w}) will occur through gas exchange and by advection and dispersion. Thus, the surface area and volume exposed to the atmsophere will change. In these cases, a second tracer is necessary. Although a nonvolatile tracer would be advantageous for this purpose, because its decrease in concentration over time would be affected only by advection and dispersion, no tracer with the appropriate detection limit that is adequately inert has been found for large-scale ocean work.

For large-scale work, a clever alternative has been found in which two gases with different diffusion coefficients are used, namely ^{3}He and SF_6 (Watson et al. 1991, Wanninkhof et al. 1993). The light isotope of helium, ^{3}He, meets the same criteria of inertness, low background, and low detection limits as SF_6. ^{3}He has a Sc number that is eight times smaller than SF_6. When the two gases are released in a constant ratio, their concentration decrease in the water column due to dispersion will be the same but the loss due to gas exchange will be different and this difference will be proportional to the inverse square root of the ratio of their respective Sc numbers: $(\mathrm{Sc}_{^3\mathrm{He}}/\mathrm{Sc}_{\mathrm{SF6}})^{-1/2}$ (i.e., ^{3}He will be removed more quickly by gas exchange than SF_6 because it transfers three times faster through the water surface). The gas transfer velocity of ^{3}He, $k(^3\mathrm{He})$ can then be expressed as

$$k(^3\mathrm{He}) = \frac{-h}{\Delta t}\Delta\left\{\ln\left(\frac{[^3\mathrm{He}]}{[\mathrm{SF}_6]}\right)\right\}\left\{1-\left[\frac{\mathrm{Sc}(^3\mathrm{He})}{\mathrm{Sc}(\mathrm{SF}_6)}\right]^{1/2}\right\}^{-1}, \tag{18}$$

where the delta term in braces represents the change in the logarithm of the ratio of the gas concentrations over the time interval Δt. ^{3}He is one of the few gases that will work in combination with SF_6 for this application, because the Sc numbers for other candidate gases are similar to that of SF_6 (**Table 1**).

Successful ^{3}He/SF_6 studies have been performed in several different ocean basins under a range of conditions (Nightingale et al. 2000b, Ho et al. 2006, Wanninkhof et al. 2004). The time interval to determine k will depend on the rate of gas transfer and mixed layer depth, and ranges from one to four days. Results of most dual deliberate tracer studies over the ocean plotted versus wind speed are shown in **Figure 3**.

Proxy Techniques

Inertial dissipation method. The challenges associated with the eddy correlation method for the estimation of fluxes at sea have led to the use of the inertial dissipation method in the atmospheric boundary layer (Fairall & Larsen 1986). The method assumes an approximate balance of the generation and dissipation of turbulent fluctuations of the concentration of the gas whose flux is to be measured. This method is based on MOST for the high-frequency portion of the variance, or concentration fluctuation, spectrum. The method has been used extensively to measure drag coefficients over the open ocean (Yelland et al. 1994).

The concentration variance budget in the atmospheric boundary layer can be expressed as

$$-\overline{C'w'}\left(\frac{\partial C}{\partial z}\right) - \frac{1}{2}\frac{\partial\overline{C'^2w}}{\partial z} = \varepsilon_c. \tag{19}$$

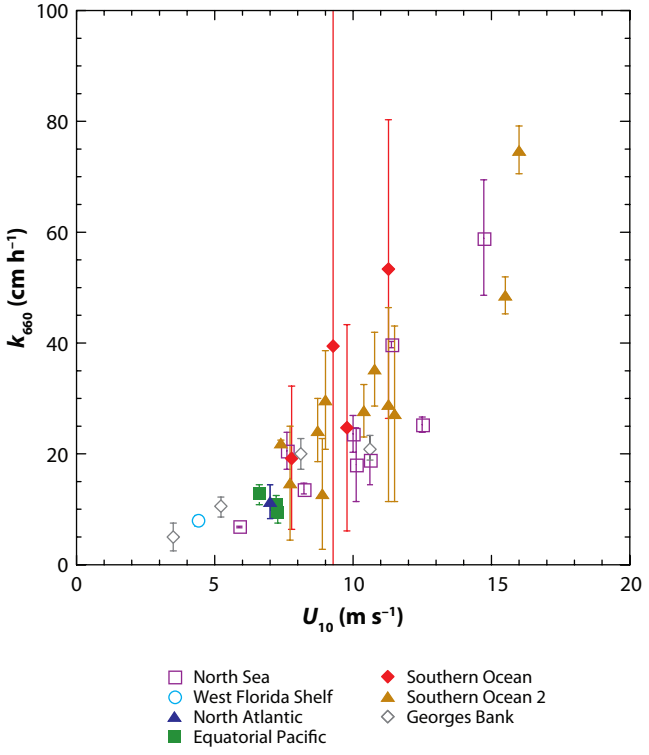

Figure 3

Summary of ^{3}He/SF$_6$ dual-deliberate tracer results normalized to Sc = 660 and plotted against wind speed. The open symbols are for the experiments in the coastal oceans, while the solid symbols depict the studies in the open ocean. The error bars are based on the variation of ^{3}He/SF$_6$ in the mixed layer at each sampling time propagated through Equation 18. References are as follows: North Sea, Nightingale et al. (2000b); West Florida Shelf, Wanninkhof et al. (1997); North Atlantic, Wanninkhof & McGillis (1999); Equatorial Pacific, Nightingale et al. (2000a); Southern Ocean, Wanninkhof et al. (2004); Southern Ocean 2, Ho et al. (2006); Georges Bank, Wanninkhof et al. (1993).

The first term is the rate of production of concentration fluctuations that arise from the action of the turbulent flux ($C'w'$) on the gradient of concentration $\partial C/\partial z$. The middle term is the divergence of fluctuations, or transport term, and is generally accounted for by corrections based on similarity relations between fluxes and scalar gradients. The last term, the rate of turbulent kinetic dissipation, ε_c, is the rate of destruction of these fluctuations due to molecular diffusivity and is believed to approximately balance the production term (Edson & Fairall 1998). The rate of turbulent kinetic dissipation, ε_c, is then related to the mean square gradients of the concentration. The idea of separation of the large scales of production from the small scales of dissipation leads to a high-frequency region of the gas variance spectrum that follows –5/3 in frequency. The level reflects the cascade toward molecular dissipation at higher frequencies. As with the atmospheric profile technique, the inertial dissipation technique requires the use of MOST because the boundary layer stability conditions change the structure of the atmospheric turbulence.

In the inertial dissipation technique, the gas flux F requires the variance spectrum of gas concentration and MOST to get c_* and the friction velocity u_{a*},

$$F = c_* u_{a*}. \tag{20}$$

By equating dissipation to generation and knowing the dependence of the overall gradient of concentration, the gas transfer rate may be determined. Some work has been done in applying this method to gas fluxes over the ocean for CO_2 (Larsen et al. 1997). The main attraction of the inertial dissipation method is its use of the high-frequency portion of the spectrum where platform motions are much smaller than the turbulence signal. Thus, ship motion corrections and precise vertical alignments are not required. However, the inertial subrange occurs at frequencies higher than the upper frequency limit of the covariance method, so this method requires a very fast sensor response and the requirements for low sensor noise are more critical.

Heat. Heat is an attractive proxy tracer of air-water gas exchange because temperature can be measured with high accuracy and very good temporal resolution (Jähne et al. 1989), thus allowing the details of air-water exchange to be studied. With the advent of infrared (IR) imagers, especially those equipped with focal plane arrays, several so-called IR thermographic techniques have been developed that allow the spatial details of air-water heat exchange to be measured with unprecedented spatial and temporal resolution (Haußecker & Jähne 1995; Haußecker et al. 1995, 2002; Garbe et al. 2004; Schimpf et al. 2004).

The use of IR thermographic methods for the study of gas transfer relies on the assumption that the net flux of heat and the resulting transfer velocity, k(heat), can be related to an equivalent value for gas via the use of a diffusivity scaling based on Equation 6. Although initial applications of the technique indicated that this scaling worked and a direct equivalence existed between k(heat) and k(gas) (Jähne et al. 1989, Haußecker et al. 1995), more recent use of heat as a proxy tracer has indicated that the relationship might not be as straightforward as implied by Equation 6. In particular, Zappa and coworkers (2004), Atmane and coworkers (2004), and Asher and coworkers (2004) all find that when scaled according to Equation 6, k(heat) measured by the active infrared technique developed by Haußecker and colleagues (1995) overpredicts k(gas) by a factor of two to three. Similarly, Garbe and coworkers (2004) find a scale factor of 1.3 between k(heat) and k(gas). Atmane and coworkers (2004) explain this scale factor as a result of the interplay between the distance at which water-side turbulence eddies approach the interface and the order of magnitude difference in diffusive length scales between heat and gas. There is scientific debate as to whether thermographic techniques provide a means for definitive quantification of k(gas), and a clear resolution to this problem is not available at present. However, whatever the final resolution of the question of a direct equivalence between k(heat) and k(gas), it is clear that IR imagery provides a unique means to visualize the microscale wave breaking, coherent motions, and aqueous-phase turbulence occurring very near the water surface.

RECENT FIELD STUDIES THAT UTILIZE IMPROVED MEASUREMENT TECHNIQUES

Major advances have been made in determining k over the ocean in several large field campaigns such as the GasEx-98 and GasEx-2001 studies (McGillis et al. 2001, 2004b), the Air-Sea Gas Exchange/Marine Aerosol and Gas Exchange (ASGAMAGE) field program (Jacobs et al. 2002), and the Surface Ocean Lower Atmosphere Study (SOLAS) Air-Sea Gas Exchange (SAGE) experiment (Ho et al. 2006). These studies successfully addressed the challenges outlined above. For direct flux measurements, improvements include accurate correction for the ship's motion (Edson et al. 1998), improved sensor resolution, accurate assessments of Webb corrections, and performing studies in regions with a sufficient concentration gradient to improve the signal-to-noise ratio. These studies have dealt with all the shortcomings of the direct flux techniques outlined in Broecker et al. (1986). New analysis techniques have facilitated DMS flux measurements from

ships (Huebert et al. 2004). Although errors in individual 10–30 min direct flux measurements still are 50–100%, the effective use of statistical approaches, with the large numbers of observations such as bin averaging in discrete wind speed ranges, has decreased the uncertainty in binned measurements to 10% over two to four weeks of sampling.

Determination of k from water column mass balance estimates is now almost exclusively done by dual-deliberate tracer methods that use ^{3}He and SF_6. Improved accuracy and speed of analysis of SF_6, an increased number of measurements of ^{3}He at shoreside laboratories, and improved sampling protocols have all contributed to greater accuracy of the measurements. The uncertainty of the measurements is a direct function of measurement interval; longer intervals lead to greater decreases in ratios (Equation 18) but also generally lead to integration over larger ranges of wind speed. Accurate determination of ratio decrease depends on good estimates of the mixed layer depth. Precisions of better than 10% over one- to two-day intervals have been achieved by the dual tracer method over the ocean (Ho et al. 2006). Studies relating the dual tracer results to other gases have been performed (Asher & Wanninkhof 1998), but additional efforts are warranted considering the increased use of this approach. These additional efforts are necessary because for CO_2, sea spray and bubble injection due to breaking waves and to a lesser extent to rainfall may affect the dependence of k on Sc number given in Equation 18.

FORCING

Most determinations of gas transfer velocities are complex and require dedicated field studies. To utilize the gas transfer velocities to determine regional or global fluxes through bulk formulations such as given in Equation 1, the measurements must be scaled up and/or parameterized with forcing functions that can be readily determined. Here, we first describe gas transfer and forcing over a smooth or undulated surface, and then extend it to situations where bubbles affect the exchange.

The general expression for gas transfer is given by Equation 6. Relating the function $f(Q, L, \nu)$ to environmental forcing becomes the key issue. Based on analogous behavior between heat, momentum, and gas, the surface friction velocity in water, u_{w*}, is a critical parameter (Jähne et al. 1987). Deacon (1977) proposed a general formulation for k in the case of an aerodynamically smooth surface,

$$k = \beta^{-1} u_{w*} \mathrm{Sc}^{-n}, \tag{21}$$

where β is a numerical constant determined from classical boundary layer theory. Although this representation can account for shear-induced turbulence in the absence of waves, it is not appropriate when there is significant contribution to the net stress from breaking and nonbreaking waves or when other drivers such as bubble entrainment, rain, and buoyancy-generated turbulence are significant.

An alternative approach is to establish a formulation that includes most parameters known to affect gas exchange. This was performed by Fairall and coworkers (2000) and Hare and coworkers (2004) and leads to the following expression for sparingly soluble gases with liquid-side control:

$$k = u_{a*}[(\rho_w/\rho_a)^{-1/2}(h_w \,\mathrm{Sc}_w^{1/2} + \ln(z_w/d_w)/\kappa)]^{-1}, \tag{22}$$

where subscripts w and a refer to the water and air phase, respectively, and ρ_a and ρ_w are the density of air and water, respectively. $h_w = \Lambda R_r^{1/4}/\varphi$, where Λ is an adjustable parameter, R_r is the roughness Reynolds number, and φ is an empirical function that accounts for buoyancy effects on turbulent transfer. Many of the variables in Equation 22 can be estimated from knowledge of air and water temperature, sea surface skin temperature, salinity, net long-wave and short-wave radiation, wind speed, relative humidity, and atmospheric pressure. However, the absolute magnitudes of

the fluxes are determined from fitting results from field studies. The integrated model developed by Hare and coworkers (2004) includes the effect of bubbles on k, which are added as a separate component (see below). The parameters included in Equation 22 clearly indicate that simple equations that relate gas transfer with wind lack the full range of parameters that affects gas transfer.

Relationships of Gas Exchange With Wind

Many factors can affect gas transfer, but over the global ocean wind forcing has a dominant effect. This phenomenon has a theoretical foundation based on the relationship of k and u_* (see Equations 21 and 22) and the relationship between wind and friction velocity, which under neutral atmospheric conditions is

$$U_{10} = (\rho_w/\rho_a)^{1/2} u_{w*} C_d^{-1/2}, \tag{23}$$

where C_d is the drag coefficient that is related to the surface roughness. The u_{w*} is the friction velocity in water and is related to the friction velocity in air, u_{a*}, through $u_{w*} = (\rho_a/\rho_w)^{1/2}\, u_{a*}$.

Although theoretical relations between U_{10} and u_{w*} exist for all atmospheric stabilities, most relationships of k with wind are empirical. The first successful studies that related gas exchange to wind were performed in wind-wave tunnels followed by deliberate tracer studies in lakes. Although a general trend of k increasing with increases in U_{10} was observed over the ocean with the mass balance techniques that use O_2 and ^{222}Rn, it was not until the advent of the dual deliberate tracer methods that clear patterns of gas transfer with wind over the ocean were observed (**Figure 3**).

The first popular gas exchange–wind speed parameterization was derived from conceptual and theoretical considerations adjusted to the natural environment. On the basis of theoretical arguments and wind-wave tanks results, Liss & Merlivat (1986) assumed three linear segments of gas transfer with wind: the smooth regime, a regime with an undulating surface, and a regime with breaking waves. The relationship for the undulating regime Equation 25 was adjusted so that k_{600} matched the first deliberate tracer results from lakes (Wanninkhof et al. 1985),

$$k_{600} = 0.17\ U_{10} \qquad (U_{10} < 3.6\ \text{m s}^{-1}), \tag{24}$$

$$k_{600} = 2.85\ U_{10} - 9.65 \qquad (3.6 < U_{10} < 13\ \text{m s}^{-1}), \tag{25}$$

$$k_{600} = 5.9\ U_{10} - 49.3 \qquad (U_{10} > 13\ \text{m s}^{-1}), \tag{26}$$

where 600 in k_{600} refers to the Sc of CO_2 at 20°C for fresh water. The k_{600} (and k_{660} below) are expressed in cm h^{-1} and U_{10} is expressed in m s^{-1}. Wanninkhof (1992) used the global bomb ^{14}C constraint (Broecker et al. 1985) and wind-wave tank results, and suggested that k scaled with U_{10}^2 (Wanninkhof & Bliven 1991). The quadratic dependence is in accord with theory suggesting that gas transfer scales with wind stress, τ, where $\tau = C_d U_{10}^2$ such that $k \approx a U_{10}^2$. The relationship scaled to global bomb ^{14}C is

$$k_{660} = 0.39 \langle U_{10} \rangle^2, \tag{27}$$

where k_{660} is the Sc number of CO_2 at 20°C for seawater (Wanninkhof 1992). This curve also was a good fit through the Red Sea bomb ^{14}C estimates (Cember 1989). It was recognized that if this long-term constraint was used for shorter timescales the wind variability had to be taken into account, which leads to a relationship for steady or short-term winds with a coefficient of 0.31, that is, $k_{660} = 0.31\ \langle U_{10}^2 \rangle$. The popularity of this relationship hinges in large part on the fact that it yielded consistent results when applied to numerical global ocean biogeochemistry models that used the same global bomb ^{14}C constraint/criteria for circulation and carbon mass balance estimates (Sarmiento & LeQuere 1996). In contrast, the relationship of Liss & Merlivat (1986) yields global fluxes that are approximately 50% lower.

A synthesis of dual deliberate tracer studies by Nightingale and colleagues (2000b) provided the first estimates of global transfer velocities based on local studies (**Figure 3**). The experiments used by Nightingale and colleagues (2000b) were performed in fetch limited environments (coastal seas) and although it is not clear if this introduces a bias in the resulting parameterization, the encouraging aspect is that studies from a wide range of locations provided a clear trend with wind that was parameterized as

$$k_{600} = 0.333\ U_{10} + 0.222\ U_{10}^2. \tag{28}$$

In fact, several subsequent efforts listed below suggest convergence toward dependencies similar to those of Nightingale and colleagues (2000b). Sweeney and coworkers (2007) followed up on earlier suggestions that the bomb ^{14}C inventory estimated by Broecker and colleagues (1989, 1995) was approximately 25% too high (Hesshaimer et al. 1994, Peacock 2004) and performed a more robust analysis that used inverse modeling to deduce that the gas transfer–wind speed relationship was approximately 33% lower than the estimate in Wanninkhof (1992). Ho and colleagues (2006) performed a deliberate tracer study with ^3He and SF_6 in the Southern Ocean near New Zealand that included measurements at high wind (up to 16 m s^{-1}) that was parameterized according to

$$k_{600} = 0.266\ U_{10}^2, \tag{29}$$

which agrees well with the parameterizations of Sweeney and colleagues (2007) and Nightingale and coworkers (2000b). The commonality of these global algorithms is that they all are quadratic, have a zero intercept, and are implicitly applicable to all sparingly soluble gases.

Although the concordance between the quadratic parameterizations is encouraging, they are at odds with an increasing body of evidence that over the ocean k will not go to zero at low wind speeds but will rather asymptote to a finite value owing to buoyancy effects and, in the case of CO_2, chemical enhancement. For most ocean studies there is little observational data for $U_{10} <$ 4 m s^{-1} such that results are extrapolated to zero, in part because studies in wind-wave tanks with fresh water show k_{CO_2} of < 1 cm h^{-1} for quiescent conditions. The direct flux measurements have provided more data at low winds over the ocean and clearly suggest a nonzero trend. McGillis and coworkers (2001, 2004b) use an asymptote of 3 cm h^{-1} to fit data for a study in the North Atlantic and 8 cm h^{-1} for the equatorial Pacific, respectively. In the latter study, McGillis and coworkers (2004b) suggested the large enhancement is due to buoyancy fluxes associated with a strong diurnal heating cycle.

Studies have shown a large enhancement of gas fluxes due to breaking waves and bubble entrainment (Wallace & Wirick 1992; Farmer et al. 1993; Asher et al. 1996, 1997; Zhang et al. 2006; McNeil & d'Asaro 2007). The transfer through bubbles is complex and, in addition to the noted dependence on Sc, α becomes a controlling factor in the exchange, with low solubility gases experiencing a greater enhancement than gases with higher solubility (Memery & Merlivat 1986). Further complications arise because of the asymmetry in the bubble-mediated gas flux with bubble-driven gas fluxes for invasion being higher than evasive bubble fluxes (Memery & Merlivat 1986).

The contribution to the flux that is due to bubbles is frequently parameterized as an additive component to the flux through the unbroken surface so that (Woolf 2005)

$$F_{Total} = F_i + F_b, \tag{30}$$

where F_{Total} is the total gas flux, F_i is the flux through the unbroken surface, and F_b is the bubble-mediated gas flux. The gas transfer due to bubbles has been argued to scale with the fractional ocean surface area coverage by whitecaps, W, which in turn scales roughly to U_{10}^3 (Monahan & Spillane 1984). Using the bulk air-water concentration difference in Equation 30 then permits the

net transfer velocity k to be expressed as an area weighted average given by

$$k = k_i(1 - W) + k_b W, \tag{31}$$

where k_i is the transfer velocity through the unbroken surface and k_b is the bubble-mediated transfer velocity. Although modeling studies (Memery & Merlivat 1986, Woolf & Thorpe 1991, Woolf 2005) and laboratory measurements (Asher et al. 1996, 1997; Komori & Misumi 2002; Woolf et al. 2007) have attempted to determine a function form for k_b in terms of physicochemical variables, its precise definition remains elusive.

Despite the fact that the details of k_b are unknown, it is possible to study the dependence of k on breaking waves using the available field data. Using the GasEx-98 dataset, McGillis and coworkers (2001) assumed that the observed increase in k with U_{10} was controlled by breaking waves and that k_i was constant with U_{10}. These assumptions lead to a functional form for k given by $k = a + b\ U_{10}^3$, assuming $W \ll 1$. This is a reasonable assumption because $W \approx 0.02$ for $U_{10} \approx 20\ \mathrm{m\ s^{-1}}$ (for instance, Asher et al. 2002). Using this functional form, McGillis and coworkers (2001) found that for the GasEx-98 data, k could be parameterized by:

$$k_{660} = 3.3 + 0.026\ U_{10}^3, \tag{32}$$

with a similar result for the data from the GasEx-2001 experiment (McGillis et al. 2004b):

$$k_{660} = 8.2 + 0.014\ U_{10}^3. \tag{33}$$

The relationships, along with the binned data, are shown in **Figure 4**. Using a similar approach as that used with the GasEx-98 dataset, Asher and coworkers (2002) found excellent agreement between the oceanic k values and those predicted from a whitecap-based model via the use of an empirically derived functional form for k_b and measured values for W. However, a caution must be placed on assuming Equations 32, 33, or the parameterization given by Asher and coworkers (2002) represent a general relation for whitecap-driven gas transfer. Because the GasEx-98 dataset is for CO_2 invasion and the GasEx-2001 dataset is for evasion, and because a known asymmetry exists between invasion and evasion when bubble-mediated processes are important, the relations discussed here apply only to these specific cases. Overall, although it is understood that whitecaps play an important role in air-sea gas transfer, especially at high wind speeds, accurate parameterization of this effect remains elusive.

Issues in The Use of Gas Exchange–Wind Speed Relationships

When using gas exchange–wind speed relationships to calculate regional or global-scale fluxes, it is important to use consistent winds. Global mean wind speed estimates can differ by more than 1 m s^{-1} (Boutin et al. 2002, Naegler et al. 2006). For instance, the NCEP assimilated product yields a global average wind of 6.6 m s^{-1} and the global average QuikSCAT satellite winds are 7.9 m s^{-1} (Naegler et al. 2006), which will result in biases in global CO_2 fluxes of $(7.9/6.6)^2$ or 43% for quadratic dependencies and $(7.9/6.6)^3$ or 71% for cubic relationships (Wanninkhof et al. 2002). Spatial distributions of winds are not consistent among different wind speed climatologies either. In particular, the mean U_{10} in the equatorial Pacific region can differ by as much as 2 m s^{-1} depending on which climatological wind speed is used. C. Sweeney (unpublished data) demonstrates with a numerical model that although the bomb ^{14}C constraint yields consistent global mean gas transfer velocities for different wind speed climatologies, the relative difference in wind speeds in the Equatorial and Southern oceans yields a difference in global mean air-sea CO_2 flux of 0.5 Pg $year^{-1}$ (or ~25%) using a quadratic dependence between k and U_{10}.

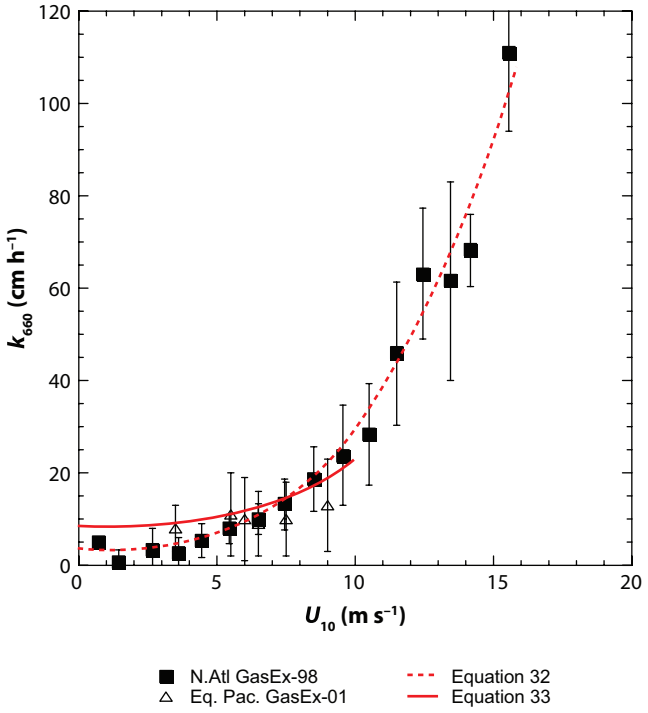

Figure 4

Comparison of CO_2 covariance flux measurements in the North Atlantic (*solid squares*) (McGillis et al. 2001) and Equatorial Pacific (*open triangles*) (McGillis et al. 2004b, Hare et al. 2004). The results are binned in nominally 1 m s^{-1} wind speed bins and the error bars indicate the standard deviation of the points in each interval that range from as few as 4 at low and high winds to more than 200 at intermediate winds. The dashed red line is the parameterization expressed in Equation 32 and the solid red line is that in Equation 33.

Another issue is how to apply the relationships correctly over temporal and spatial scales with varying winds. If the instantaneous gas transfer is expressed as

$$k_{inst} = a U_{10}^n, \tag{34}$$

the average k, k_{av}, over the time intervals will be $k_{av} = a\langle U_{10}^n \rangle = a\sigma^n$, where σ^n is the nth moment. For $n = 2$, σ^2 is the variance, and for $n = 3$, σ^3 is the skewness of the wind speed distribution. The global wind speed distribution can be represented as a Rayleigh distribution function (Wentz et al. 1984), in which case the k_{av} will be 27% higher than the k_{inst} for a quadratic relationship and 91% higher for a cubic relationship at a particular wind speed. These issues are often overlooked and contribute to the discrepancies in comparisons of different flux estimates.

Other Types of Forcing

From first principles and observations, wind by itself clearly does not control transfer across the interface but rather affects the turbulence. Other mechanisms can affect turbulence at the interface. Here we briefly describe friction velocity, bubbles, buoyancy fluxes, energy dissipation, fetch, surface slicks, rain, and chemical enhancement as additional or complementary factors that affect gas transfer velocities.

Friction velocity is a better environmental variable to estimate gas transfer than wind because it is intrinsically related to turbulence at the water surface. Several of the first-order parameterizations (see Equations 21 and 22) are expressed in terms of friction velocity. Large & Pond (1981) provide a full description of the relationship between U_{10} and u_{a*} for different environmental conditions. For low winds and neutral stability, they determined that C_d is invariant, whereas at intermediate winds C_d scales linearly with wind speed. The relationship between U_{10} and u_{a*} will vary depending on wave state and surfactant concentrations. Erickson (1993) derived relationships that incorporate boundary layer stability as it affects u_{a*} into his parameterizations.

At low winds, it is not only u_{a*}, but also buoyancy fluxes that will affect surface turbulence. Buoyancy fluxes are not readily parameterized without a full knowledge of heat and momentum fluxes but can be included in parameterizations as outlined by Fairall et al. (2000) (see Equation 22). On the basis of direct flux measurements of CO_2 in the equatorial Pacific, these effects can be significant in areas with high heat fluxes (McGillis et al. 2004b).

An alternative perspective suggests that gas exchange is controlled by the dissipation of energy at the surface rather than stress or u_{a*}. Several controlled studies provide support for this concept (Asher & Pankow 1986, Zappa et al. 2007). The practical implication of this suggestion is that the dissipation scales roughly to the cube of the wind, which lends support for strongly nonlinear dependencies of k on U_{10}.

Irrespective of the mechanism of gas transfer, it is clear that wave field will strongly affect the exchange. Therefore, fetch, the distance the winds blow over the ocean, is believed to have a first-order effect on the transfer. Results of field studies using eddy correlation techniques show a fetch effect for ozone (Fairall et al. 2006). Theoretical work by Woolf (2005) suggests that the effect is significant for fetches up to 1000 km in large part because of development of breaking wave fields and contributions by bubbles to gas transfer.

Bubble effects are often considered additive to transfer across the air-water interface (see Equations 30 and 31). Bubbles can greatly enhance the exchange of gases across the air-sea interface by extreme turbulence associated with wave breaking and the rise of the plume back to the surface, and by transfer of gases through the walls of individual bubbles. In the latter case, the solubility of the gas becomes an important factor; lower solubility gases experience a greater bubble enhancement than gases with greater solubility. Studies suggest that the enhancement by bubbles can be scaled roughly to the cube of the wind with a strong solubility dependence (Asher et al. 2002). Woolf (1997) estimated that bubbles contribute 30% of the global gas transfer velocity of CO_2. The exact magnitude of the effect of bubbles on gas transfer, and CO_2 fluxes in particular, remains an active resesearch area but there is general consensus that bubbles play a first order role in gas transfer.

Surfactants inhibit the exchange primarily through inhibition of surface turbulence (Frew 1997). Wind-wave tank results show that surfactants at very low concentrations retard gas transfer at the highest wind speeds studied, suggesting that gas exchange in the ocean is for practical purposes always affected by naturally occurring surfactants. Surfactants decrease the gas exchange and also u_{w*} under a smooth surface regime such that decreases in k scale with decreases in u_{w*}. The decreases in k at higher winds/turbulent conditions are more difficult to quantify with forcing. The retardation of the net air-sea CO_2 flux over the ocean due to surfactants is estimated to be as large as 20% to 50% based on the laboratory results and remotely sensed data of the effects of surfactants on waves, and estimates of surfactant concentrations due to biological productivity (Tsai & Liu 2003). However, Asher (1997) concluded that surfactants would actually increase the net CO_2 flux because the effects are most pronounced in regions with low winds where the direction of CO_2 flux is out of the ocean (**Figure 5**). The widely divergent results indicate the uncertainty of the surfactant effect on gas transfer and CO_2 fluxes over the ocean.

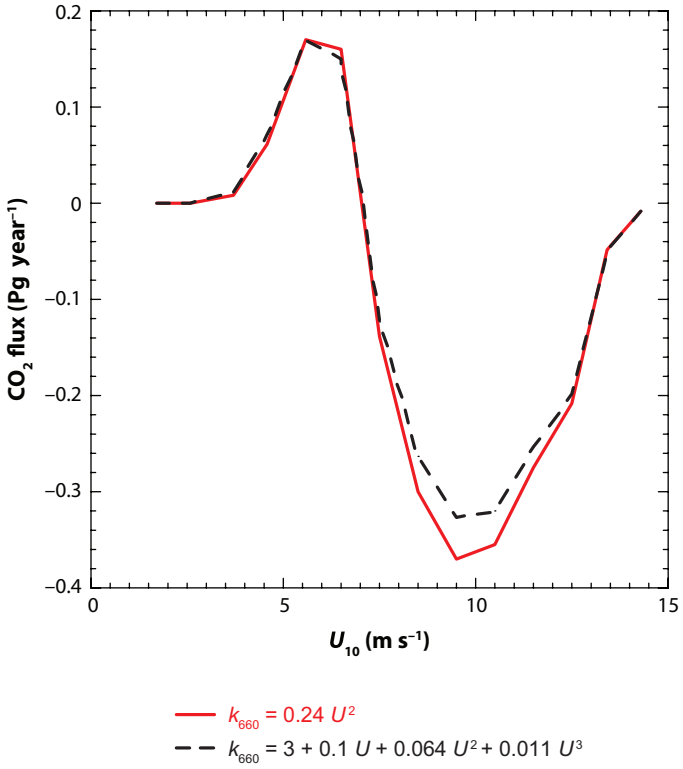

Figure 5

Global CO_2 flux plotted against wind speed. The solid red line is the quadratic dependence and the dashed black line is the polynomial dependence from **Figure 6**, both constrained by the global k from bomb ^{14}C. The ΔpCO_2 field is from Takahashi et al. (2008) and winds used are the average QuikSCAT winds for 2000–2004.

Rain has a large effect on the gas transfer velocity. Controlled studies show that k is related to rain rate and drop size. Both of these parameters can be expressed in terms of a kinetic energy flux, momentum flux, or energy dissipation (Ho et al. 1997, 2004; Takagaki & Komori 2007). The effect is predominantly caused by increased turbulence at the surface, whereas bubbles introduced by impinging raindrops are a secondary effect (Ho et al. 2000), likely because of the shallow penetration of rain-induced bubbles. The effect of rain can contribute appreciably to the total exchange in certain regions with high rain rates such as the western equatorial Pacific and Bay of Bengal during the monsoon season. However, when rainfall is integrated over the entire globe, it plays a secondary effect on gas transfer. Komori and coworkers (2007) have estimated that the effect of rain on CO_2 exchange on the global scale is less than 5%.

CO_2 can react with hydroxide ions in the molecular boundary layer to form bicarbonate, thereby enhancing gas transfer. The enhancement has been estimated in several studies with similar results, and results are in agreement with theoretical calculations if the appropriate hydration constants are used (Johnson 1982). Chemical enhancement has a relatively small effect on global scale. Because the reactions are temperature dependent, the enhancement will be most pronounced in tropical regions. Globally, the effect is believed to be less than 3% (Wanninkhof & Knox 1996).

TOWARD RECONCILIATION

A clear picture is emerging of which factors are important in controlling k. However, these effects have not been fully incorporated in models to determine global flux fields, in part because there has been little evidence that incorporation of comprehensive surface forcing provides a better flux field than simple wind speed algorithms. The release of improved global forcing fields using

remote sensing offers an opportunity to make meaningful advances. Algorithms can be established that utilize the direct returns from remotely sensed products, or products derived from remote sensing, data assimilation, and/or modeling can be used.

Surface water concentration climatologies of several gases are currently available (for instance, for DMS, Kettle & Andreae 2000). However, these climatologies lack comprehensive data coverage and often rely on bold temporal and spatial extrapolations. The most comprehensive observation-based global climatology of pCO_2 is that of Takahashi and colleagues (2008). The surface water pCO_2 fields are derived from approximately three million surface water observations used in combination with a surface flow field from a general circulation model to determine pCO_2 on a 4° by 5° grid with monthly resolution. Mole fractions of CO_2 in air are obtained from a well-constrained interpolated global dataset (Coop. Atmos. Data Integr. Proj. 2007), which, combined with ambient pressure, yields the pCO_2 in air. The k is determined from wind speed assuming a quadratic dependence that is scaled to the revised global bomb ^{14}C constraint (Sweeney et al. 2007). The derived global net flux into the ocean of 1.6 Pg C year^{-1} is in good agreement with the global estimate of anthropogenic CO_2 uptake obtained from independent mass balance and isotopic methods of 2.2 Pg C year^{-1} when accounting for a riverine flux of 0.4 Pg C year^{-1} and for the fact that the climatology is for a non–El Niño year. The inclusion of El Niño years is thought to contribute on average an additional 0.2 Pg C year^{-1} to the flux estimate, yielding a total anthropogenic flux (= net flux + riverine input + El Niño contribution) of 2 Pg C year^{-1} by this method. The uncertainty is estimated at 0.7 Pg C year^{-1} with approximately 30% attributed to the uncertainty in the coefficient between k and U_{10}^2 and 20% attributed to uncertainty in the winds. However, these rough uncertainty estimates do not necessarily account for regional biases and compensating errors. Advances in quantifying the forcing of gas exchange on global scales offers an opportunity to provide more robust estimates of k.

To create a global flux product, variability in both the concentration fields and forcing must be accounted for at grid scales at least as small as the concentration field grid. Wind speed has been the forcing field of choice because of its availability on a global scale for many applications, including ocean modeling. It is not clear, however, that wind speed is actually the best representation of surface turbulence. The near-synoptic coverage offered through satellite remote sensing provides attractive opportunities to determine forcing, not only because it is at the appropriate resolution, but also because satellite observations of the sea surface wave slope may be a better direct measurement of turbulence than wind speed. The wave slope is determined from satellite sensors using specific wavebands that represent surface roughness at 10–30-cm scales. Glover and coworkers (2002) took advantage of the strong correlation between wave slope and k along with wave slope information from altimeters to estimate global k at high resolution. Altimeters provide good information on waves but have global coverage on a 10-day repeat cycle, thereby missing temporal variability (Frew et al. 2007). Scatterometers provide significantly better coverage, but obtaining meaningful wave slope information from their wide swath is challenging. The global k fields obtained in this fashion appear to underestimate the k at high winds, likely because the effect of bubbles is not implicitly included in their algorithms. Refinements of the approach are underway but it is not clear if the fidelity of the k versus wave slope algorithms derived from altimetry and/or scatterometry is superior to the relationships with wind speed derived from the same sensors.

Another approach is to use a model that incorporates the processes known to affect the gas transfer, taking advantage of the global surface fields of wind stress, heat, and momentum such as provided by the National Centers for Environmental Prediction (NCEP). The derivation by Fairall and coworkers (2000) (Equation 22) offers good opportunities in this respect, in particular when the effects of bubbles and chemical enhancement are included as extra terms. The scalable

coefficients can be adjusted via the use of global constraints such as the carbon isotopes. Efforts are underway to provide global estimates of k that utilize the global surface forcing databases (G. Wick & C. Fairall, personal communcation).

Although simple parameterizations with wind cannot capture all the processes that control gas transfer, it appears that they can capture most processes under neutral or unstable boundary conditions that are prevalent over much of the ocean. The common characterizations are either quadratic or cubic dependencies. The use of nonzero intercepts to account for zero wind speed gust environments or zero wind-driven processes are less frequently included. From a mechanistic standpoint, the quadratic dependencies suggest that gas exchange is roughly related to surface stress or the momentum flux at the ocean surface. The cubic dependencies suggest that energy dissipation plays a key role in the control of gas transfer rates at low to intermediate winds and that bubbles enhance the exchange at higher winds. The degree to which these processes affect gas exchange is explored using a hybrid model following the approach of Woolf (2005) with the form

$$k_{660} = a + b\langle U_{10}\rangle + c\langle U_{10}^2\rangle + d\langle U_{10}^3\rangle. \quad (35)$$

Nightingale and colleagues (2000b) have proposed a similar parameterization for a synthesis of dual deliberate tracer results but without the intercept or cubic term (see Equation 28). The linear term is in support of the original work of Deacon (1977), who provided an expression of gas exchange that is linear with u_{w^*} at low winds. Because the drag coefficient is constant at low winds, U_{10} is linearly related to u_{w^*} in this range.

Equation 35 cannot be constrained a priori by a single global bomb ^{14}C inventory estimate, so we utilize information from the literature to estimate the coefficients a, b, and d. Coefficient c is then determined from the global bomb ^{14}C constraint. The value of a will be dependent on the buoyancy flux and chemical enhancement. The average chemical enhancement of CO_2 exchange over the ocean (pH = 8, sea surface temperature = 18°C) is calculated at 2.3 cm h^{-1}. The average buoyancy flux that is unrelated to u_{w^*} is guessed to be 0.7 cm h^{-1} to yield a nonzero intercept of 3 cm h^{-1}, which is approximately the lower limit of k observed in field studies. The second coefficient is determined from the relationship developed by Deacon (1977) and involves converting u_{a*} to U_{10} assuming $C_d = 1.2\ 10^{-3}$. We obtain a coefficient b of 0.1 that makes the resulting 0.1 $\langle U_{10}\rangle$ term negligible compared with the intercept. The coefficient for the cubic is 0.011, assuming the relationship of CO_2 exchange with whitecap coverage is linear and using wind speed–whitecap coverage relationships as outlined in Woolf (2005). However, here we scale whitecap coverage to U_{10}^3 rather than $U_{10}^{3.41}$, which was suggested in Woolf (2005). As a final step, the coefficient for the quadratic term is determined via the use of the average global k revised bomb ^{14}C inventory of 17 cm h^{-1} (Naegler et al. 2006), and wind speeds and moments from the QuikSCAT satellite wind product for 2000–2004. The global bomb ^{14}C constraint has been recently reassessed by several authors (Sweeney et al. 2007, Krakauer et al. 2006, Naegler et al. 2006), and they obtained k_{av} ranging from 15–21 cm h^{-1}. The average QuikSCAT winds and moments derived for monthly averages on a 4° by 5° grid, excluding coastal areas and ice-covered regions as used in the Takahashi climatology, are as follows: average wind speed, $\langle U_{10}\rangle$, is 7.68; the second moment, $\langle U_{10}^2\rangle$, is 71.95; and the third moment, $\langle U_{10}^3\rangle$, is 783.4. This yields a coefficient c of 0.064, resulting in a final equation of

$$k_{660} = 3 + 0.1\langle U_{10}\rangle + 0.064\langle U_{10}^2\rangle + 0.011\langle U_{10}^3\rangle. \quad (36)$$

The k_{660} derived from Equation 36 and the individual terms are plotted in **Figure 6**. The quadratic expression that fits the global constraint of 17 cm h^{-1} is presented as well. In the hybrid relationship, the cubic term dominates at intermediate to high winds (>8 m s^{-1}), whereas the

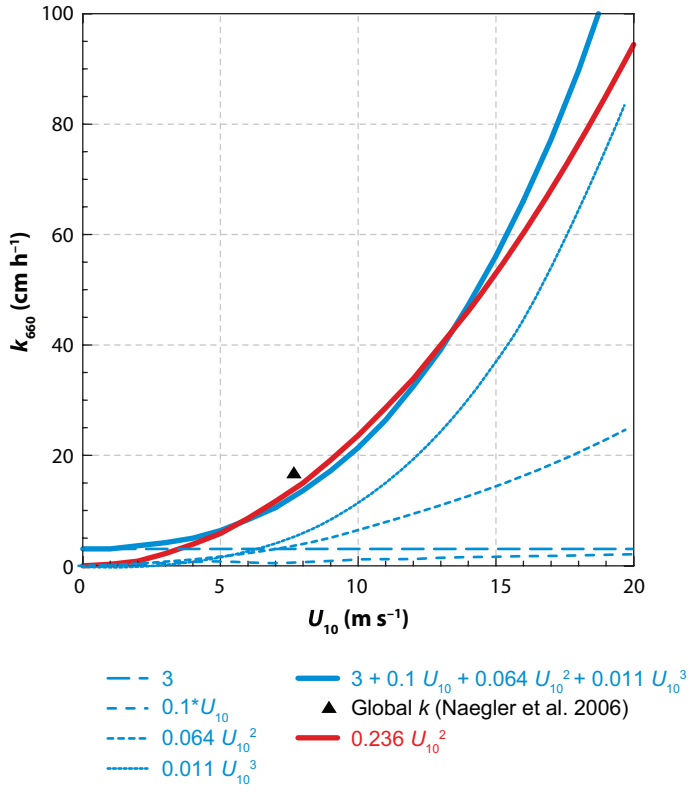

Figure 6

Comparison of the polynomial function with wind (Equation 36) (*blue line*) with a quadratic (Equation 37) (*red line*), all constrained by the average k from bomb ^{14}C (Naegler et al. 2006). The dashed lines are the individual terms in Equation 36 listed in the legend.

constant term dominates at winds of less than 3 m s^{-1}. However, a quadratic fit that meets the global constraint is nearly indistinguishable from the hybrid form for winds <15 m s^{-1},

$$k_{660} = 0.24\langle U_{10}^2 \rangle. \quad (37)$$

Considering that for a global Rayleigh wind distribution 96% of the winds are below 15 m s^{-1}, a simple quadratic dependence appears, at first glance, adequate for an empirical relationship (**Figure 6**).

To determine the difference between the polynomial expression and a quadratic function in global CO_2 flux estimates, we apply the parameterizations of Equations 36 and 37 to the CO_2 climatology of Takahashi and coworkers (2008). Equation 37 yields an uptake of –1.3 Pg C year^{-1}, whereas the polynomial expression (Equation 36) gives a net uptake of –1.14 Pg C year^{-1}, or a 15% difference. The distribution of fluxes is plotted against monthly mean wind speed in **Figure 5**. The slightly lower dependence of Equation 36 compared with Equation 37 at winds between 6

and 12 m s^{-1} leads to a lower CO_2 flux into the ocean. This result emphasizes the need for accurate parameterizations.

The effect of different wind speed relationships on global CO_2 fluxes is as follows: For the same functional dependencies, the global CO_2 flux will scale proportionally with the coefficients if the same wind speed product is used. Different functional dependencies, even if they are scaled to the same global mean k fluxes, can yield significantly different CO_2 fluxes. Higher-order dependencies generally exhibit lower global CO_2 uptake because they yield lower k at intermediate winds (≈6–10 m s^{-1}) that are prevalent over the ocean and because most of the flux into the ocean is within these wind speed ranges (**Figure 5**).

SUMMARY POINTS

1. The application of direct flux meteorological techniques to measure gas fluxes makes it possible to measure fluxes at the same time and space scales as the environmental forcing processes.
2. Micrometeorological approaches have put the gas transfer on a sound theoretical foundation through invoking similarity with heat and momentum fluxes.
3. Infrared imaging techniques have improved the understanding and quantification of near-surface turbulence on small scales.
4. Satellite remote sensing and data assimilation provide comprehensive global fields of environmental forcing, including wind, sea surface temperature, air temperature, and friction velocity.
5. Dual deliberate tracer studies provide a means to quantify k at any desired locale with timescales on the order of a day.
6. A wind speed–only polynomial function is developed to determine the gas transfer velocity that can be well approximated by a conventional quadratic function for the prevalent wind speed range. However, the small difference in functionality at intermediate winds has an appreciable effect on the calculated global CO_2 fluxes.
7. The role of breaking waves at high wind speeds is recognized as important, but as yet there remains no reliable way to accurately quantify the effect of breaking waves on gas exchange.

DISCLOSURE STATEMENT

The authors are not aware of any biases that might be perceived as affecting the objectivity of this review.

ACKNOWLEDGMENTS

Discussions with participants of the K-Conundrum Workshop sponsored by the Surface Ocean-Lower Atmosphere Study (SOLAS) and the European Union COST Program in Norwich, United Kingdom in February 2008 were very beneficial in producing this work. We appreciate the expert copyediting and proofreading by Gail Derr of NOAA/AOML.

Appendix A

List of Symbols

α	Ostwald solubility coefficient (nondimensional)	F_i	Flux through the unbroken surface
δ	Thickness of the stagnant film	h	Water depth that is in contact with air; defined as V/A (mixed layer depth)
ε	Chemical enhancement factor	I	Deficit of ^{222}Rn relative to ^{226}Ra in the mixed layer
ε_c	Turbulent kinetic energy dissipation	k	Gas transfer velocity
εk_w	Gas transfer velocities of the gas through the diffusive sublayer layers on the water side	k_{660}	Gas transfer velocity normalized to a Sc number of 660
k_a/α	Gas transfer velocities of the gas through the diffusive sublayer on the air side	k_{av}	Average gas transfer velocity
Λ	Adjustable parameter	k_b	Bubble-mediated transfer velocity
ν	Kinematic viscosity of water	k_i	Transfer velocity through the unbroken surface
σ_w	Standard deviation of vertical velocity	k_{inst}	Instantaneous gas transfer velocity
φ	Empirical function that accounts for buoyancy effects on turbulent transfer	K_o	Aqueous-phase solubility
λ	Radioactive decay constant	L	Turbulence integral length scale
κ	Von Karman constant (≈0.4)	M	Mass of gas in water
ρ_a	Density of air	pCO_{2a}	Partial pressure of CO_2 in air
ρ_w	Density of water	pCO_{2w}	Partial pressure of CO_2 in water
σ^n	(Statistical) n^{th} moment	Q	Velocity scale
^{222}Rn	Isotope of radon	R	Ideal gas constant
^{226}Ra	Isotope of radium	$R_{1,2}$	Transfer resistance between the heights of measurement in air
^{3}He	Light isotope of helium	R_{air}	Air-side resistance to gas transfer
a	Constant	R_r	Roughness Reynolds number
A	Radioactive activity	R_{water}	Water-side resistance to gas transfer
A	Surface area	S	Sources or sinks other than the air-sea flux
$b\chi$	Parameter that depends on the threshold and characteristic length scales of turbulence	Sc	Schmidt number (nondimensional)
c'	Fluctuations of gas concentration about a mean	SF_6	Sulfur hexafluoride
C_d	Drag coefficient	T_W	Water temperature
C_a	Concentration of the gas in the air	U	Wind speed
C_o	Gas concentration at the water surface	$u*$	Water-side friction velocity
C_w	Gas concentration in the well-mixed bulk fluid below the surface	U_{10}	Wind speed at 10-m height under neutral boundary conditions
C_{z1}	Concentration at height z_1 in the atmospheric boundary layer	u_{a*}	Friction velocity in air
D	Molecular diffusivity	u_{w*}	Surface friction velocity in water
F	Air-sea gas flux	V	Water volume
F_b	Bubble-mediated gas flux	W	Fractional white cap coverage
		w	Vertical velocity

LITERATURE CITED

Asher WE. 1997. The sea surface microlayer and its effect on global air-sea gas transfer. See Liss & Duce 1997, pp. 251–86

Asher WE, Edson JB, McGillis WR, Wanninkhof R, Ho DT, Litchendorf T. 2002. Fractional area whitecap coverage and air-sea gas transfer velocities measured during GasEx-98. See Donelan et al. 2002, pp. 199–204

Asher WE, Farley PJ, Higgins BJ, Karle LM, Monahan EC, Leifer IS. 1996. The influence of bubble plumes on air/seawater gas transfer velocities. *J. Geophys. Res.* 101:12027–41

Asher WE, Jessup AT, Atmane MA. 2004. Oceanic application of the active controlled flux technique for measuring air-sea transfer velocities of heat and gases. *J. Geophys. Res.* 109:C08S12

Asher WE, Karle LM, Higgins BJ. 1997. On the differences between bubble-mediated air-water gas transfer in freshwater and seawater. *J. Mar. Res.* 55:813–45

Asher WE, Pankow JF. 1986. The interaction of mechanically generated turbulence and interfacial films with a liquid phase controlled gas/liquid transport process. *Tellus B* 38:305–18

Asher WE, Pankow JF. 1989. Direct observation of concentration fluctuations close to a gas/liquid interface. *Chem. Eng. Sci.* 44:1451–55

Asher WE, Wanninkhof R. 1998. Transient tracers and air-sea gas transfer. *J. Geophys. Res.* 103:15939–58

Atmane MA, Asher WE, Jessup AT. 2004. On the use of the active infrared technique to infer heat and gas transfer velocities at the air-water free surface. *J. Geophys. Res.* 109:C08S14

Banerjee S, Lakehal D, Fulgosi M. 2004. Surface divergence models for scalar exchange between turbulent streams. *Int. J. Multiph. Flow* 30:963–73

Blomquist BW, Fairall CW, Huebert BJ, Kieber DJ, Westby GR. 2006. DMS sea-air transfer velocity: direct measurements by eddy covariance and parameterization based on the NOAA/COARE gas transfer model. *Geophys. Res. Lett.* 32:L07601

Bock EJ, Hara T, Frew NM, McGillis WR. 1999. Relationship between air-sea gas transfer and short wind waves. *J. Geophys. Res.* 104:25821–32

Borges AV, Wanninkhof R. 2007. Preface: 37th International Liege Colloquium on Ocean Dynamics, Liege, Belgium, May 2–6, 2005, 5th International Symposium on Gas Transfer at Water Surfaces. *J. Mar. Sys.* 66:1–3

Boutin J, Etcheto J, Merlivat L, Rangama Y. 2002. Influence of gas exchange coefficient parameterisation on seasonal and regional variability of CO_2 air-sea fluxes. *Geophys. Res. Lett.* 29(8):1182

Broecker HC, Peterman J, Siems W. 1978. The influence of wind on CO_2 exchange in a wind wave tunnel, including the effects of monolayers. *J. Mar. Res.* 36:595–610

Broecker WS, Ledwell JR, Takahashi T, Weiss R, Merlivat L, et al. 1986. Isotopic versus micrometeorologic ocean CO_2 fluxes: A serious conflict. *J. Geophys. Res.* 91(C9):10517–27

Broecker WS, Peng T-H, Östlund G, Stuiver M. 1985. The distribution of bomb radiocarbon in the ocean. *J. Geophys. Res.* 99:6953–70

Broecker WS, Sutherland S, Smethie W, Peng T-H, Östlund G. 1995. Oceanic radiocarbon: separation of the natural and bomb components. *Glob. Biogeochem. Cycles* 9:263–88

Brumley BH, Jirka GH. 1988. Air-water transfer of slightly soluble gases: turbulence, interfacial processes and conceptual models. *Phys. Chem. Hydrodyn.* 10:295–319

Brutsaert W, Jirka GH, ed. 1984. *Gas Transfer at Water Surfaces*. Hingham, MA: Reidel. 639 pp.

Businger JA, Delaney AC. 1990. Chemical sensor resolution required for measuring surface fluxes by three common micrometeorological techniques. *J. Atmos. Chem.* 19:399–410

Cember R. 1989. Bomb radiocarbon in the Red Sea: a medium-scale gas exchange experiment. *J. Geophys. Res.* 94:2111–23

Chang WN, Heikes BG, Lee MH. 2004. Ozone deposition to the sea surface: chemical enhancement and wind speed dependence. *Atmos. Env.* 38:1053–59

Cooperative Atmospheric Data Integration Project—Carbon Dioxide. 2007. *GlobalView-CO_2*. Boulder, CO: NOAA ESRL. CD-ROM (also available on Internet via anonymous FTP to ftp.cmdl.noaa.gov, path: ccg/co2/GLOBALVIEW)

Craig PD, Banner ML. 1994. Modeling wave-enhanced turbulence in the ocean surface layer. *J. Phys. Oceanogr.* 24:2546–59

d'Asaro ED, McNeil C. 2007. Air-sea gas exchange at extreme winds speeds measured by autonomous oceanographic floats. *J. Mar. Res.* 66:92–109

Danckwerts PV. 1951. Significance of liquid film coefficients in gas absorption. *Ind. Eng. Chem.* 43:1460–67

Danckwerts PV. 1970. *Gas-Liquid Reactions.* New York: McGraw Hill

Davies JT. 1972. *Turbulence Phenomena: An Introduction to the Eddy Transfer of Momentum, Mass, and Heat, Particularly at Interfaces*. New York: Academic

Davies JT, Kilner AA, Ratcliff GA. 1964. The effect of diffusivities and surface films on rates of gas absorption. *Chem. Eng. Sci.* 19:583–90

Deacon EL. 1977. Gas transfer to and across an air-water interface. *Tellus* 29:363–74

Donelan MA, Drennan WM, Saltzman ES, Wanninkhof R, ed. 2002. *Gas Transfer at Water Surfaces*. Washington, DC: Am. Geophys. Union, Geophys. Monogr. 127. 383 pp.

Edson JB, Fairall CW. 1998. Similarity relationships in the marine atmospheric surface layer for terms in the TKE and scalar variance budgets. *J. Atmos. Sci.* 55:2311–28

Edson JB, Hinton AA, Prada KE, Hare JE, Fairall CW. 1998. Direct covariance flux estimates from mobile platforms at sea. *J. Atmos. Ocean. Technol.* 15:547–62

Edson JB, Zappa CJ, Ware JA, McGillis WR, Hare JE. 2004. Scalar flux profile relationships over the open ocean. *J. Geophys. Res.* 109:C08S09

Erickson DJ III. 1993. A stability-dependent theory for air-sea gas exchange. *J. Geophys. Res.* 98:8471–88

Fairall CW, Bariteau L, Grachev AA, Hill RJ, Wolfe DE, et al. 2006. Turbulent bulk transfer coefficients and ozone deposition velocity in the International Consortium for Atmospheric Research into Transport and Transformation. *J. Geophys. Res.* 111:D23S20

Fairall CW, Hare JE, Edson JB, McGillis W. 2000. Parameterization and micrometeorological measurement of air-sea gas transfer. *Bound. Layer Meteor.* 96:63–105

Fairall CW, Larsen SE. 1986. Inertial-dissipation methods and turbulent fluxes at the air-ocean interface. *Bound. Layer Meteor.* 34:287–301

Fairall CW, White AB, Edson JB, Hare JE. 1997. Integrated shipboard measurements of the marine boundary layer. *J. Atmos. Ocean. Tech.* 14:338–59

Farmer DM, McNeil CL, Johnson BD. 1993. Evidence for the importance of bubbles in increasing air-sea gas flux. *Nature* 361:620–23

Forster P, Ramaswamy V, Artaxo P, Berntsen T, Betts R, et al. 2007. Changes in atmospheric constituents and in radiative forcing. In *Climate Change 2007: The Physical Science Basis. Contribution of Working Group I to the Fourth Assessment Report of the Intergovernmental Panel on Climate Change*, ed. S. Solomon, D. Qin, M. Manning, Z. Chen, M. Marquis, et al. Cambridge, UK: Cambridge University Press.

Fortescue GF, Pearson JRA. 1967. On gas absorption into a turbulent liquid. *Chem. Eng. Sci.* 22:1162–80

Frew NM. 1997. The role of organic films in air-sea gas exchange. See Liss & Duce 1997, pp. 121–72

Frew NM, Bock EJ, Schimpf U, Hara T, Haußecker H, et al. 2004. Air-sea gas transfer: Its dependence on wind stress, small-scale roughness, and surface films. *J. Geophys. Res.* 109:C08S17

Frew NM, Glover DM, Bock EJ, McCue SJ. 2007. A new approach to estimation of global air-sea gas transfer velocity fields using dual-frequency altimeter backscatter. *J. Geophys. Res.* 112:C11003

Frew NM, Goldman JC, Dennett MR, Johnson AS. 1990. Impact of phytoplankton-generated surfactants on air-sea gas exchange. *J. Geophys. Res.* 95:3337–52

Gallagher MW, Beswick KM, Coe H. 2001. Ozone deposition to coastal waters. *Q. J. R. Meteorol. Soc.* 127:539–58

Garbe CS, Handler RA, Jähne B, ed. 2007. *Transport at the Air-Sea Interface: Measurements, Models and Parameterizations*. Berlin: Springer Verlag. 320 pp.

Garbe CS, Schimpf U, Jähne B. 2004. A surface renewal model to analyze infrared image sequences of the ocean surface for the study of air-sea heat and gas exchange. *J. Geophys. Res.* 109:C08S15

Glover DM, Frew NM, McCue SJ, Bock EJ. 2002. A multi-year time series of global gas transfer velocity from the TOPEX/POSEIDON dual frequency normalized radar backscatter algorithm. See Donelan et al. 2002, pp. 325–33

Hara T, Inwegen EV, Wendelbo J, Garbe CS, Schimpf U, et al. 2007. Estimation of air-sea gas and heat fluxes from infrared imagery based on near surface turbulence models. See Garbe et al. 2007, pp. 241–54
Hare JE, Fairall CW, McGillis WR, Edson JB, Ward B, Wanninkhof R. 2004. Evaluation of the National Oceanic and Atmospheric Administration/Coupled-Ocean Atmospheric Response Experiment (NOAA/COARE) air-sea gas transfer parameterization using GasEx data. *J. Geophys. Res.* 109:C08S11
Harriott P. 1962. A random eddy modification of the penetration theory. *Chem. Eng. Sci.* 17:149–54
Haußecker HW, Jähne B. 1995. In situ measurements of the air-sea gas transfer rate during the MBL/COOP west coast experiment. See Jähne & Monahan 1995, pp. 775–84
Haußecker HW, Jähne B, Reinalt S. 1995. Heat as a proxy tracer for gas exchange measurements in the field: principles and technical realization. See Jähne & Monahan 1995, pp. 405–13
Haußecker HW, Schimpf U, Garbe CS, Jähne B. 2002. Physics from IR image sequences: quantitative analysis of transport models and parameters of air-sea gas transfer. See Donelan et al. 2002, pp. 103–8
Hesshaimer V, Heimann M, Levin I. 1994. Radiocarbon evidence for a smaller oceanic carbon dioxide sink than previously believed. *Nature* 370:201–3
Ho DT, Asher WE, Bliven LF, Schlosser P, Gordan EL. 2000. On mechanisms of rain-induced air-water gas exchange. *J. Geophys. Res.* 105:24045–57
Ho DT, Bliven LF, Wanninkhof R, Schlosser P. 1997. The effect of rain on air-water gas exchange. *Tellus B* 49:149–58
Ho DT, Law CS, Smith MJ, Schlosser P, Harvey M, Hill P. 2006. Measurements of air-sea gas exchange at high wind speeds in the Southern Ocean: implications for global parameterizations. *Geophys. Res. Lett.* 33:L16611
Ho DT, Zappa CJ, McGillis WR, Bliven LF, Ward B, et al. 2004. Influence of rain on air-sea gas exchange: lessons from a model ocean. *J. Geophys. Res.* 109:C08S18
Huebert BJ, Blomquist BW, Hare JE, Fairall CW, Johnson JE, Bates TS. 2004. Measurement of the sea-air DMS flux and transfer velocity using eddy correlation. *Geophys. Res. Lett.* 31:L23113
Jacobs C, Nightingale P, Upstill-Goddard R, Kjeld JF, Larsen S, Oost W. 2002. Comparison of the deliberate tracer method and eddy covariance measurements to determine the air/sea transfer velocity of CO_2. See Donelan et al. 2002, pp. 225–31
Jähne B, Haußecker H. 1998. Air-water gas exchange. *Ann. Rev. Fluid Mech.* 30:443–68
Jähne B, Huber W, Dutzi A, Wais T, Ilmberger J. 1984. Wind/wave-tunnel experiment on the Schmidt number and wave field dependence of air/water gas exchange. See Brutsaert & Jirka 1984, pp. 303–9
Jähne B, Libner P, Fischer R, Billen T, Plate EJ. 1989. Investigating the transfer process across the free aqueous viscous boundary layer by the controlled flux method. *Tellus B* 41:177–95
Jähne B, Monahan EC, ed. 1995. *Air-Water Gas Transfer: Selected Papers from the Third International Symposium on Air-Water Gas Transfer*. Hanau, Germany: Aeon Verlag. 900 pp.
Jähne B, Münnich KO, Bösinger R, Dutzi A, Huber W, Libner P. 1987. On the parameters influencing air-water gas exchange. *J. Geophys. Res.* 92:1937–49
Johnson KS. 1982. Carbon dioxide hydration and dehydration kinetics in seawater. *Limnol. Oceanogr.* 27:849–55
Katsaros KB, Smith SD, Oost WA. 1987. HEXOS-humidity exchange over the sea: a program for research on water-vapor and droplet fluxes from sea of air at moderate to high wind speeds. *Bull. Am. Meteorol. Soc.* 68:466–76
Kettle AJ, Andreae MO. 2000. Flux of dimethylsulfide from the oceans: a comparison of updated data sets and flux models. *J. Geophys. Res.* 105:26793–808
Komori S, Misumi R. 2002. The effects of bubbles on mass transfer across the breaking air-water interface. See Donelan et al. 2002, pp. 285–90
Komori S, Takagaki N, Saiki R, Suzuki N, Tanno K. 2007. The effect of raindrops on interfacial turbulence and air-water gas transfer. See Garbe et al. 2007, pp. 169–79
Krakauer NY, Randerson JT, Primau FW, Gruber N, Menemenlis D. 2006. Carbon isotope evidence for the latitudinal distribution and wind speed dependence of the air-sea gas transfer velocity. *Tellus B* 58:390–417
Kromer B, Roether W. 1983. Field measurements of air-sea gas exchange by the radon deficit method during JASIN 1978 and FGGE 1979. "*Meteor*" *Forsch. Ergebnisse A/B* 24:55–75
Lamont JC, Scott DS. 1970. An eddy cell model of mass transfer into the surface of a turbulent liquid. *Am. Inst Chem. Eng. J.* 16:513–19

Large WP, Pond S. 1981. Open ocean momentum flux measurements in moderate to strong winds. *J. Phys. Oceanogr.* 11:324–36

Larsen SE, Hansen FA, Kjeld JF, Lund SW, Kunz G, deLeeuw G. 1997. Experimental and modeling study of air-sea exchange of carbon dioxide. *Proc. ASGAMAGE Workshop*, ed. WA Oost, pp. 116–23. De Bilt, The Netherlands: Royal Dutch Meteor. Inst.

Ledwell J. 1984. The variation of the gas transfer coefficient with molecular diffusivity. See Brutsaert & Jirka 1984, pp. 293–303

Lee YH, Luk S. 1982. Characterization of concentration boundary layer in oxygen absorption. *Ind. Eng. Chem. Fundam.* 21:428–34

Lenchow DH, Pearson R, Stankov BB. 1982. Measurements of ozone vertical flux to ocean and forest. *J. Geophys. Res.* 87:8833–37

Liss PS. 1983. Gas transfer: experiments and geochemical implications. In *Air-Sea Exchange of Gases and Particles*, ed. PS Liss, WG Slinn, pp. 241–99. Dordrecht, The Netherlands: Reidel

Liss PS, Duce RA, ed. 1997. *The Sea Surface and Global Change*. Cambridge, UK: Cambridge Univ. Press. 535 pp.

Liss PS, Heimann M, Roether W. 1988. Tracers of air-sea gas exchange (and discussion). *Phil. Trans. R. Soc. London Ser. A Math. Phys. Sci.* 325:93–103

Liss PS, Merlivat L. 1986. Air-sea gas exchange rates: introduction and synthesis. In *The Role of Air-Sea Exchange in Geochemical Cycling*, ed. P Buat-Menard, pp. 113–29. Boston, MA: Reidel

Liss PS, Slater PG. 1974. Fluxes of gases across the air-sea interface. *Nature* 247:181–84

Liu H. 2005. An alternative approach for CO_2 flux correction caused by heat and water vapour transfer. *Bound. Layer Meteor.* 115:151–68

Luk S, Lee YH. 1986. Mass transfer in eddies close to an air-water interface. *Am. Inst. Chem. Eng. J.* 32:1546–54

McCready MJ, Hanratty TJ. 1984. Concentration fluctuations close to a gas-liquid interface. *Am. Inst. Chem. Eng. J.* 30:816–17

McCready MJ, Hanratty TJ. 1985. Effect of air-shear on gas absorption by a liquid film. *Am. Inst. Chem. Eng. J.* 34:2066–78

McGillis WR, Asher WE, Wanninkhof R, Jessup AT, Feely RA. 2004a. Introduction to special section: Air-sea exchange. *J. Geophys. Res.* 109:C08S01

McGillis WR, Dacey JWH, Frew NM, Bock EJ, Nelson BK. 2000. Water-air flux of dimethylsulfide. *J. Geophys. Res.* 105:1187–93

McGillis WR, Dacey JWH, Ware JD, Ho DT, Bent JT, et al. 2007. Air-water flux reconciliation between the atmospheric CO_2 profile and mass balance techniques. See Garbe et al. 2007, pp. 181–92

McGillis WR, Edson JB, Hare JE, Fairall CW. 2001. Direct covariance of air-sea CO_2 fluxes. *J. Geophys. Res.* 106:16729–45

McGillis WR, Edson JB, Zappa CJ, Ware JD, McKenna SP, et al. 2004b. Air-sea CO_2 exchange in the equatorial Pacific. *J. Geophys. Res.* 109:C08S02

McNeil CD, d'Asaro E. 2007. Parameterization of air-sea gas fluxes at extreme wind speeds. *J. Mar. Sys.* 66:110–21

Memery L, Merlivat L. 1986. Modeling of the gas flux through bubbles at the air-water interface. *Tellus B* 37:272–85

Monahan EC, Spillane MC. 1984. The role of oceanic whitecaps in air-sea gas exchange. See Brutsaert & Jirka, 1984, pp. 495–503

Münsterer T, Jähne B. 1998. LIF measurements of concentration profiles in the aqueous mass boundary layer. *Exp. Fluids* 25:190–96

Naegler T, Ciais P, Rodgers K, Levin I. 2006. Excess radiocarbon constraints on air-sea gas exchange and the uptake of CO_2 by the oceans. *Geophys. Res. Lett.* 33:L11802

Najjar RG, Keeling RF. 1997. Analysis of the mean annual cycle of the dissolved oxygen anomaly in the World Ocean. *J. Mar. Res.* 55:117–51

Nie D, Kleindienst TE, Arnts RR, Sickles JE. 1995. The design and testing of a relaxed eddy accumulation system. *J. Geophys. Res.* 100:11415–23

Nightingale PD, Liss PS, Schlosser P. 2000a. Measurements of air-sea gas transfer during an open ocean algal bloom. *Geophys. Res. Lett.* 27:2117–20

Nightingale PD, Malin G, Law CS, Watson AJ, Liss PS, et al. 2000b. In situ evaluation of air-sea gas exchange parameterizations using novel conservative and volatile tracers. *Glob. Biogeochem. Cycles* 14:373–87

Peacock S. 2004. Debate over the ocean bomb radiocarbon sink: Closing the gap. *Glob. Biogeochem. Cycles* 18:GB2022

Peng T-H, Broecker WS, Mathieu GG, Li YH, Bainbridge AE. 1979. Radon evasion rates in the Atlantic and Pacific oceans as determined during the GEOSECS program. *J. Geophys. Res.* 84:2471–86

Redfield AC. 1948. The exchange of oxygen across the sea surface. *J. Mar. Res.* 7:347–61

Roether W. 1983. Field measurement of air-sea gas transfer: a methodical search. *Bound. Layer Meteor.* 27:97–103

Sarmiento JL, LeQuere C. 1996. Oceanic carbon dioxide uptake in a model of century-scale global warming. *Science* 274:1346–50

Saylor JR, Handler RA. 1999. Capillary wave gas exchange in the presence of surfactants. *Exp. Fluids* 27:332–38

Schimpf U, Garbe CS, Jähne B. 2004. Investigation of transport processes across the sea-surface microlayer by infrared imagery. *J. Geophys. Res.* 109:C08S13

Smethie WM, Takahashi TT, Chipman DW, Ledwell JR. 1985. Gas exchange and CO_2 flux in the tropical Atlantic Ocean determined from ^{222}Rn and pCO_2 measurements. *J. Geophys. Res.* 90:7005–22

Soloviev AV, Schlussel P. 1994. Parameterization of the cool skin of the ocean and of the air-ocean gas transfer on the basis of modeling surface renewal. *J. Phys. Oceanogr.* 24:1339–46

Sweeney C, Gloor E, Jacobson AR, Key RM, McKinley G, et al. 2007. Constraining global air-sea gas exchange for CO_2 with recent bomb ^{14}C measurements. *Glob. Biogeochem. Cycles* 21:GB2015

Takagaki N, Komori S. 2007. Effects of rainfall on mass transfer across the air-water interface. *J. Geophys. Res.* 112:C06006

Takahashi T, Sutherland SC, Wanninkhof R, Sweeney C, Feely RA, et al. 2008. Climatological mean and decadal change in surface ocean pCO_2 and net sea-air CO_2 flux over the global oceans. *Deep-Sea Res.* In press

Takehara K, Etoh GT. 2002. A direct visualization method of CO_2 gas transfer at water surface driven by wind waves. See Donelan et al. 2002, pp. 89–95

Terray EA, Donelan MA, Agrawal YC, Drennan WM, Kahma KK, et al. 1996. Estimates of kinetic energy dissipation under breaking waves. *J. Phys. Oceanogr.* 26:792–806

Tsai WT, Liu KK. 2003. An assessment of the effect of sea surface surfactant on global atmosphere-ocean CO_2 flux. *J. Geophys. Res.* 108(C4):3127

Upstill-Goddard RC, Watson AJ, Liss PS, Liddicoat MI. 1990. Gas transfer velocities in lakes measured with SF_6. *Tellus B* 42:364–77

Upstill-Goddard RC, Watson AJ, Wood J, Liddicoat MI. 1991. Sulphur hexafluoride and helium-3 as sea-water tracers: Deployment techniques and continuous underway analysis for sulphur hexafluoride. *Anal. Chim. Acta* 249:555–62

Wallace DWR, Wirick CD. 1992. Large air-sea gas fluxes associated with breaking waves. *Nature* 356:694–96

Wanninkhof R. 1992. Relationship between gas exchange and wind speed over the ocean. *J. Geophys. Res.* 97:7373–81

Wanninkhof R, Asher W, Weppernig R, Chen H, Schlosser P, et al. 1993. Gas transfer experiment on Georges Bank using two volatile deliberate tracers. *J. Geophys. Res.* 98:20237–48

Wanninkhof R, Bliven LF. 1991. Relationship between gas exchange, wind speed, and radar backscatter in a large wind-wave tank. *J. Geophys. Res.* 96:2785–96

Wanninkhof R, Doney SC, Takahashi T, McGillis WR. 2002. The effect of using time-averaged winds on regional air-sea CO_2 fluxes. See Donelan et al. 2002, pp. 351–57

Wanninkhof R, Hitchcock G, Wiseman W, Vargo G, Ortner P, et al. 1997. Gas exchange, dispersion, and biological productivity on the west Florida Shelf: Results from a Lagrangian tracer study. *Geophys. Res. Lett.* 24:1767–70

Wanninkhof R, Knox M. 1996. Chemical enhancement of CO_2 exchange in natural waters. *Limnol. Oceanogr.* 41:689–98

Wanninkhof R, Ledwell JR, Broecker WS. 1985. Gas exchange-wind speed relation measured with sulfur hexafluoride on a lake. *Science* 227:1224–26

Wanninkhof R, Ledwell JR, Watson AJ. 1991. Analysis of sulfur hexafluoride in seawater. *J. Geophys. Res.* 96:8733–40

Wanninkhof R, McGillis WR. 1999. A cubic relationship between gas transfer and wind speed. *Geophys. Res. Lett.* 26:1889–93

Wanninkhof R, Sullivan KF, Top Z. 2004. Air-sea gas transfer in the Southern Ocean. *J. Geophys. Res.* 109:C08S19

Watson AJ, Upstill-Goddard RC, Liss PS. 1991. Air-sea exchange in rough and stormy seas measured by a dual tracer technique. *Nature* 349:145–47

Webb EK, Pearman GI, Leunig R. 1980. Correction of flux measurements for density effects due to heat and vapor transfer. *Q. J. R. Meteorol. Soc.* 106:85–100

Wentz FJ, Peteherych S, Thomas LA. 1984. A model function for ocean radar cross sections at 14.6 GHz. *J. Geophys. Res.* 89(C3):3689–704

Wilhelms SC, Gulliver JS. 1991. *Proceedings of the Second International Symposium on Gas Transfer at Water Surfaces.* New York: ASCE. 797 pp.

Wolff LM, Hanratty TJ. 1994. Instantaneous concentration profiles of oxygen accompanying absorption in a stratified flow. *Exp. Fluids* 16:385–92

Woodrow PT Jr, Duke SR. 2001. Laser-induced fluorescence studies of oxygen transfer across unsheared flat and wavy air-water interfaces. *Ind. Eng. Chem. Res.* 40:1985–95

Woolf DK. 2005. Parameterization of gas transfer velocities and sea-state-dependent wave breaking. *Tellus B* 57:87–94

Woolf DK. 1997. Bubbles and their role in gas exchange. In *The Sea Surface and Global Change*, ed. P.S. Liss and R.A. Duce, pp. 173-206. Cambridge, UK: Cambridge Univ. Press

Woolf DK, Leifer IS, Nightingale PD, Rhee TS, Bowyer P, et al. 2007. Modelling of bubble-mediated gas transfer: fundamental principles and a laboratory test. *J. Mar. Sys.* 66:71–91

Woolf DK, Thorpe S. 1991. Bubbles and the air-sea exchange of gases in near-saturation conditions. *J. Mar. Res.* 49:435–66

Yelland MJ, Taylor PK, Consterdine IE, Smith MH. 1994. The use of the inertial dissipation technique for shipboard wind stress determination. *J. Atmos. Ocean. Tech.* 11:1093–108

Zappa CJ, Asher WE, Jessup AT. 2001. Microscale wave breaking and air-water gas transfer. *J. Geophys. Res.* 106:9385–92

Zappa CJ, Asher WE, Jessup AT, Klinke J, Long SR. 2004. Microbreaking and the enhancement of air-water transfer velocity. *J. Geophys. Res.* 109:C08S16

Zappa CJ, McGillis WR, Raymond PA, Edson JB, Hintsa EJ, et al. 2007. Environmental turbulent mixing controls on air-water gas exchange in marine and aquatic systems. *Geophys. Res. Lett.* 34:L10601

Zemmelink HJ, Gieskes WWC, Klaassen W, de Groot HW, de Baar HJW, et al. 2002. Simultaneous use of relaxed eddy accumulation and gradient flux technique for the measurement of sea-to-air exchange of dimethyl sulphide. *Atmos. Environ.* 36:5709–17

Zemmelink HJ, Klaassen W, Gieskes WWC, de Baar HJW, de Groot HW, et al. 2004. Relaxed eddy accumulation measurements of the sea-to-air transfer of dimethylsulfide over the northeastern Pacific. *J. Geophys. Res.* 109:C01025

Zhang W, Perrie W, Vagle S. 2006. Impacts of winter storms on air-sea gas exchange. *Geophys. Res. Lett.* 33:L14803

Zhao D, Toba Y, Suzuki Y, Komori S. 2003. Effect of wind waves on air-sea gas exchange: Proposal of an overall CO_2 transfer velocity formula as a function of breaking-wave parameter. *Tellus B* 55:478–87

Annual Review of
Marine Science

Volume 1, 2009

Contents

Errata

An online log of corrections to *Annual Review of Marine Science* articles may be found at http://marine.annualreviews.org/errata.shtml